

Copyright Warning & Restrictions

The copyright law of the United States (Title 17, United States Code) governs the making of photocopies or other reproductions of copyrighted material.

Under certain conditions specified in the law, libraries and archives are authorized to furnish a photocopy or other reproduction. One of these specified conditions is that the photocopy or reproduction is not to be “used for any purpose other than private study, scholarship, or research.” If a user makes a request for, or later uses, a photocopy or reproduction for purposes in excess of “fair use” that user may be liable for copyright infringement,

This institution reserves the right to refuse to accept a copying order if, in its judgment, fulfillment of the order would involve violation of copyright law.

Please Note: The author retains the copyright while the New Jersey Institute of Technology reserves the right to distribute this thesis or dissertation

Printing note: If you do not wish to print this page, then select “Pages from: first page # to: last page #” on the print dialog screen



The Van Houten library has removed some of the personal information and all signatures from the approval page and biographical sketches of theses and dissertations in order to protect the identity of NJIT graduates and faculty.

ABSTRACT

AN INVESTIGATION OF POLYETHYLENE BEARING WEAR OF NEW JERSEY LCS® KNEE ON COBALT CHROMIUM AND TITANIUM NITRIDE TYPES

by
Lei Wang

The total knee replacement systems (TKRS) are used for the treatment of osteoarthritis and rheumatoid arthritis. Excessive wear can substantially shorten their life span.

Two tests were performed to examine the wear characteristics of tibial bearings used in TKRS. Each test consisted of six sets of Anterior/Posterior Glide Tibial Bearings each with a conical control arm. The tibial bearings were all made by UHMWPE. Three of these bearings were mounted onto a Co-Cr alloy tibial platform and Co-Cr alloy LCS® femoral component. Another three sets of bearings were mounted onto a TiN tibial platform and TiN LCS® femoral component. They were put into New Jersey Mark III Knee Simulator System. The simulator was configured to produce flexion-extension and axial rotation to simulate the normal walking gait. The tests were run at 1.6 Hz. Distilled water was used as lubrication fluid.

The test results show that the loading conditions and femoral component geometry play very critical roles. However, due to the machine problems, contamination of cooling-lubricating system, other factors related to loading conditions and femoral component geometry, the wear characteristics of the tested systems cannot be determined. In light of this test, the New Jersey Mark III Knee Simulator mechanical design and control systems need to be reviewed and corrected.

**AN INVESTIGATION OF POLYETHYLENE BEARING WEAR OF
NEW JERSEY LCS® KNEE ON COBALT CHROMIUM AND TITANIUM
NITRIDE TYPES**

by
Lei Wang

**A Thesis
Submitted to the Faculty of
New Jersey Institute of Technology
in Partial Fulfillment of the Requirements for the Degree of
Master of Science in Mechanical Engineering**

Department of Mechanical Engineering

January 1999

Blank Page

APPROVAL PAGE

AN INVESTIGATION OF POLYETHYLENE BEARING WEAR OF
NEW JERSEY LCS® KNEE ON COBALT CHROMIUM AND TITANIUM
NITRIDE TYPES

Lei Wang

Dr. Tai-Ming Chu, Thesis Advisor
Assistant Professor of Mechanical Engineering, NJIT

12/11/98

Date

Dr. Ian S. Fischer, Committee Member
Associate Professor of Mechanical Engineering, NJIT

12/11/98

Date

Dr. Rong-Yaw Chen, Committee Member
Professor of Mechanical Engineering, NJIT

12/11/98

Date

BIOGRAPHICAL SKETCH

Author: Lei Wang
Degree: Master of Science
Date: January 1999

Undergraduate and Graduate Education:

- Master of Science in Mechanical Engineering,
New Jersey Institute of Technology, Newark, NJ, 1999
- Bachelor of Science in Mechanical Engineering,
Southwest Jiaotong University, Chengdu, P. R. China, 1993

Major: Mechanical Engineering

To my beloved family

ACKNOWLEDGEMENT

I would like to express my deepest and sincere appreciation to Dr. Tai-Ming Chu, for her guidance, encouragement, friendship and moral support throughout this research. Special thanks to Dr. Ian S. Fischer, and Dr. Rong-Yaw Chen for actively participating my committee. I also wish to thank Dr. Michael J. Pappas, George Makris and Endotec Inc. for providing funding and helpful advice for this research.

I also appreciate the support from my fellow graduate students in the Laboratory of Biomechanical and Rehabilitation Research and Development.

TABLE OF CONTENTS

Chapter	Page
1 INTRODUCTION	1
1.1 Problem Statement	1
1.2 The Need	2
1.3 Objective	3
1.4 Significant	4
2 LITERATURE REVIEW.....	5
3 MATERIALS AND METHODS.....	8
3.1 Experiment Setup	8
3.1.1 Experiment Equipment	8
3.1.2 Loading Condition	11
3.1.3 Pre-process of Samples	12
3.1.4 Soak Controls	14
3.1.5 Tibial Bearings' Weight Measurement	14
3.1.6 Tibial Bearings' Thickness Measurement.....	14
3.1.7 Making of Repro-Rubber Molds	16
3.2 Simulations.....	16
3.2.1 Simulation I	16
3.2.2 Simulation II.....	17
3.3 Data Processing Strategy	17
4 RESULTS.....	21

TABLE OF CONTENTS
(Continued)

Chapter	Page
4.1 Simulation I.....	21
4.2 Simulation II.....	22
5 DISCUSSION.....	27
5.1 Bearing Volumetric Loss and Wear Rate.....	27
5.2 Loading Conditions.....	30
5.3 Femoral Component Geometry.....	34
5.4 Cooling-Lubricating Fluid Contamination.....	36
5.5 Comparison with Previous Study.....	37
6 SUMMARY.....	38
7 RECOMMENDATIONS.....	39
APPENDIX A ORIGINAL DATA FROM SIMULATION I.....	41
APPENDIX B ORIGINAL DATA FROM SIMULATION II.....	46
APPENDIX C BEARING WEIGHT LOSS vs. RUNNING CYCLES.....	51
APPENDIX D BEARING WEIGHT LOSS RATE vs. RUNNING CYCLES.....	53
REFERENCES.....	55

LIST OF TABLES

Table	Page
4.1 Thickness of Tibial Bearings at Lowest Locations	26
5.1 Averaged Radius of Femoral Components at 0°, 60°, 75° Flexion angles	35
A.1.1 Weight of Primary Bearings	41
A.1.2 Weight of Control Arms	41
A.1.3 Weight of Primary Bearings	41
A.1.4 Weight of Control Arms	41
A.2.1 Weight of Primary Bearings	42
A.2.2 Weight of Control Arms	42
A.2.3 Weight of Primary Bearings	42
A.2.4 Weight of Control Arms	42
A.3.1 Weight of Primary Bearings	43
A.3.2 Weight of Control Arms	43
A.3.3 Weight of Primary Bearings	43
A.3.4 Weight of Control Arms	43
A.4.1 Weight of Primary Bearings	44
A.4.2 Weight of Control Arms	44
A.4.3 Weight of Primary Bearings	44
A.4.4 Weight of Control Arms	44
A.5.1 Weight of Primary Bearings	45
A.5.1 Weight of Primary Bearings	45

**LIST OF TABLES
(Continued)**

Table	Page
A.5.3 Weight of Primary Bearings	45
A.5.4 Weight of Control Arms	45
B.1.1 Weight of Primary Bearings.....	46
B.1.2 Weight of Control Arms	46
B.1.3 Weight of Primary Bearings.....	46
B.1.4 Weight of Control Arms	46
B.2.1 Weight of Primary Bearings.....	47
B.2.2 Weight of Control Arms	47
B.2.3 Weight of Primary Bearings.....	47
B.2.4 Weight of Control Arms	47
B.3.1 Weight of Primary Bearings.....	48
B.3.2 Weight of Control Arms	48
B.3.3 Weight of Primary Bearings.....	48
B.3.4 Weight of Control Arms	48
B.4.1 Weight of Primary Bearings.....	49
B.4.2 Weight of Control Arms	49
B.4.3 Weight of Primary Bearings.....	49
B.4.4 Weight of Control Arms	49
B.5.1 Weight of Primary Bearings.....	50
B.5.2 Weight of Primary Bearings.....	50

LIST OF TABLES
(Continued)

Table	Page
B.5.3 Weight of Primary Bearings.....	50
B.5.4 Weight of Control Arms	50
C.1 Primary Bearing Weight Loss vs. Running Cycles	51
C.2 Primary Bearing Weight Loss vs. Running Cycles.....	52
D.1 Primary Bearing Weight Loss Rate vs. Running Cycles.....	53
D.2 Primary Bearing Weight Loss Rate vs. Running Cycles.....	54

LIST OF FIGURES

Figure	Page
3.1 LCS A/P Glide Mobile Bearing Knee System.....	8
3.2 New Jersey Mark III Knee Simulator	9
3.3 Comparison of Normal Walking Profile and Simulated Load Profile	12
3.4 Sample Mounted in a Test Cell.....	13
4.1.1 Bearing Volumetric Loss vs. Running Cycles.....	23
4.1.2 Bearing Wear Rate in Volume.....	23
4.1.3 Bearing Wear Rate	24
4.2.1 Bearing Volumetric Loss vs. Running Cycles.....	24
4.2.2 Bearing Wear Rate in Volume.....	25
4.2.3 Bearing Wear Rate	25
5.1.1 Wear Rate of the 1 st and 2 nd Samples.....	29
5.1.2 Wear Rate of the 3 rd and 4 th Samples.....	29
5.1.3 Wear Rate of the 5 th and 6 th Samples	30
5.2.1 Loading Conditions of the 1 st Station.....	32
5.2.2 Loading Conditions of the 2 nd Station.....	32
5.2.3 Loading Conditions of the 3 rd Station	33
5.2.4 Comparison of Loading Conditions	34
5.3 Femoral Component Geometry Comparison.....	36
C.1 Primary Bearing Weight Loss vs Running Cycles.....	51
C.2 Primary Bearing Weight Loss vs. Running Cycles	52

LIST OF FIGURES
(Continued)

Figure	Page
D.1 Primary Bearing Weight Loss vs Running Cycles.....	53
D.2 Primary Bearing Weight Loss vs. Running Cycles.....	54

CHAPTER 1

INTRODUCTION

1.1 Problem Statement

At an estimated rate of 600,000 operations per year, joint replacement is second only to dental reconstruction as an invasive treatment of the body. [1] In case of the joint replacement, joints such as shoulders, elbows, ankles, and wrists only make up a small percentage of all joint replacement surgery. The majority is performed on the knees and hips. [2]

Prosthetic joints can be used for treatment of many disorders. And joint replacements are frequently performed to treat osteoarthritis and rheumatoid arthritis. Excessive wear in joint replacement system can substantially shorten their life span. [3] Although recent research indicates certain potential to reduce wear by applying a metal-on-metal material couple than a metal-on-polyethylene bearing, the metal-on-polyethylene bearings are still the dominant material couple in the market. [4] The reasons are listed below. First of all, metal on metal is far more expensive. [4] Secondly, neither metal on metal nor the ceramic on ceramic have the cushioning (shock absorbing) effect that the polyethylene does. [5] And finally, although polyethylene is arguably the most potent particle in the osteolysis cascade, other particles of appropriate size, such like polymethylmethacrylate and barium sulfate, can also cause osteolysis. [5] So the osteolysis is not an issue only related to the polyethylene debris but related to number and size of any of wear debris.

One issue that must be indicated is that the polyethylene mentioned here refers to Ultrahigh Molecular Weight Polyethylene (UHMWPE). Originally Charnley used High Density Polyethylene was changed to this type material mainly because UHMWPE has better abrasion resistance, strength, resistance to deformation, and fatigue strength. [6]

In addition, the polyethylene wear debris will cause aseptic loosening and late infection. [2] Aseptic loosening is a common long-term complication resulting in prosthesis failure. Morphologic features of aseptic loosening include the development of a fibrohistiocytic membrane at the bone-implant interface and periprosthetic osteolysis. Local accumulation of particulate debris followed by migration and activation of inflammatory cell (macrophages, lymphocytes, and fibroblasts) result in the release of pro-inflammatory mediators. In addition, particulate debris may also suppress osteoblast function so that overall bone loss is increased. [7] Consequently the aseptic loosening and late infection will lead a failure in the total knee joint replacement. [8]

1.2 The Need

One way to obtain information of wear of prosthetic joints is clinical follow up. It works very well when dealing the issues like the function maintenance, pain relief, and visible wear of the joint couples and so on. However, the clinical follow up cannot demonstrate the invisible wear of the joint couples and always requires several years and even tens of years. The implanted prosthetic joint could not be taken out for a detailed retrieval unless it fails and needs a revision or the patient passed away. Furthermore for a new design of joint replacement system, it would be much more difficult to obtain such information by a practical clinical follow up. As an alternative method, experimental test or simulation has

an advantage over practical clinical follow up. It can be performed to test prosthetic joints in case of wear characterization. Since the simulation test is performed on continually running mechanical equipment, related information such as wear can be gained in a relatively short time. And the test samples can be taken out of the test stations for retrieval according to a pre-selected schedule.

1.3 Objective

The overall objective of the experimental study is to examine the wear characteristics of polyethylene tibial bearings in total knee replacement system. Specifically, the study would (1) determine the wear characteristics of UHMWPE against cobalt chromium (Co-Cr) alloy and (2) the wear characteristics of UHMWPE against titanium nitride (TiN) alloy.

The current simulation was conducted on the New Jersey Mark III Knee Simulator System. Two simulations were made, with 1.9 million cycles in the first simulation and 3.7 million cycles in the second simulation. The test samples consist of six sets of Anterior/Posterior (A/P) Glide Tibial Bearings. Three sets of the bearing systems were mounted onto cobalt chromium (Co-Cr) alloy tibial platform with cobalt chromium (Co-Cr) alloy LCS® femoral component. The other three sets of the bearing were mounted onto a titanium (Ti) alloy tibial platform with LCS® femoral component and both of them were coated with titanium nitride (TiN) alloy. The geometric design of those two types of total knee replacement systems is the same. However the materials used for the metal components or their coatings are different.

Former simulation test on total hip replacement system showed that the polyethylene bearings which was against titanium nitride (TiN) alloy femoral head

presented less wear than that against cobalt chromium (Co-Cr) alloy. [9] So the specific aims of this experimental study is to compare the wear characteristics of the above two types in the total knee replacement systems.

1.4 Significant

The experimental study supported pertinent information about tibial bearings, which were against titanium nitride (TiN) alloy coated femoral, and tibial components, and tibial bearings, which were against cobalt chromium (Co-Cr) alloy femoral and tibial components. That information can be used in the future design of the total knee replacement system. A well-designed total knee replacement system could have stronger resistance property to wear. So the life span of the implant could be elongated. The patients will benefit from that improvement.

CHAPTER 2

LITERATURE REVIEW

There are two main types of knee simulation. One type of simulation is performed on a real human knee that is always from cadaver. This type of test is performed in a dynamic joint testing apparatus. It can be used to study knee joint kinematics and kinetics. The principle goal is to have flexible control over both muscle and vertical load profiles such that known loads can be applied first to intact then to surgically altered specimens. Then the effects of the surgery can be assessed based on changes in kinematics and joint reaction forces.

Another type of simulation performed on a knee joint prosthesis. The simulation includes flexion-extension, axial rotation and roll back of the femoral component on the tibial component. The simulation can support pertinent information of the knee joint prosthesis, especially about the wear character of the polyethylene bearing. The characterization of the wear becomes very important because the polyethylene debris were shown to play a significant role in macrophage recruitment and subsequent osteolysis. This particular simulation is performed on the New Jersey Mark III Knee Simulator. That simulator can support all the necessary motions for a knee joint prosthesis simulation.

An article was published in May 1990. In the article, Dr. M. J. Pappas, G. Makris, and F. F. Buechel manifested their simulation on hip joint prosthesis. They compared the wear of UHMWPE cups articulating with cobalt chromium and titanium nitride coated titanium femoral heads. A four station joint simulator was used to study the articulation of 32-mm femoral heads against UHMWPE cups. Four cobalt chromium and four titanium

nitride coated titanium heads were tested. A 2,200N fluctuating loads was applied over 70° of motion, simulating the motion and forces during normal walking. The test was run at 6 Hz in water at 37°C. A polyethylene bearing sample was immersed in the same water used for lubrication and cooling. The test was run for 10 million cycles. The test results showed that titanium nitride coating was substantially superior to cobalt chromium as an articulating surface for UHMWPE.

Although the test sample and loading condition were different between a total hip joint replacement system and a total knee joint replacement system. The above simulation still can be considered as one of factors that concludes the titanium nitride coating might have greater wear resistance than that of the cobalt chromium alloy.

Alessandro F. Canonaco [1995] performed two simulations on total knee joint replacement systems. Those two tests were conducted to examine the wear characteristics of tibial bearings used in total knee replacement systems. The first simulation tested six UHMWPE bearings on Co-Cr tibial platform and femoral components, with an off-center load applied to the bearing by the femoral component 25° from the articulating surface segment tangent. The second simulation tested three Hylamer® and three UHMWPE bearings on Co-Cr tibial platform and femoral components with a center load. The simulations were performed on New Jersey Mark III knee simulator too. The first simulation with off-center load deduced no conclusion because of machine problem. The second simulation addressed different bearing materials against same metal components, including femoral components and tibial platforms. Three Hylamer® and three UHMWPE tibial bearings were mounted into the New Jersey Mark III knee simulator. An extra pair of Hylamer® and UHMWPE bearing were used as soak controls. The weight change due

to fluid absorption can be determined by weighing those controls. The saline was used as cooling-lubrication fluid. The simulator was configured to produce flexion from 0° to 70° and axial rotation of $+6^\circ$ to -6° to simulate normal gait. The femoral mount was designed to produce an anterior-posterior motion of the bearing of about 1cm. The test ran at 2 Hz with saline being sprayed between articulating surfaces. The Hydraulic Cylinder Subsystem load was set to vary from 0 to 2,200N. For this test the load varied from 0 to 2,200 N as well. The simulation was run for 5 million cycles. The test result showed that the UHMWPE bearings have a considerably lower wear rate than those of Hylamer® bearings.

The simulation conducted presently was run on the same knee simulator as that of Alessandro F. Canonaco [2]. The key differences are that the former test addressed different bearing materials on same metal components and current study addressed same bearing material in different metal. Moreover, the loading profile is different from that of the previous study. Both tests address a comparison between plastic-metal joint pairs.

The current simulation test has been planned to run for 10 million cycles. It is as two times as the former test. The information, a long-term wear characters of polyethylene bearings, should be obtained after 5 million cycles. It is very useful because the patients tend to be more and more vivid. Their expectation for a long life span of knee joint prosthesis becomes stronger and stronger. In the current simulation, two pressure sensors instead of one were used at the same time when setting up the loading profile. That might minimize the difference in the loading profile between simulation stations.

CHAPTER 3

MATERIALS AND METHODS

3.1 Experiment Setup

3.1.1 Experiment Equipment

The current experimental test is performed to examine the wear characteristics of tibial bearings used in the New Jersey LCS® total knee replacement systems (Figure 3.1). The

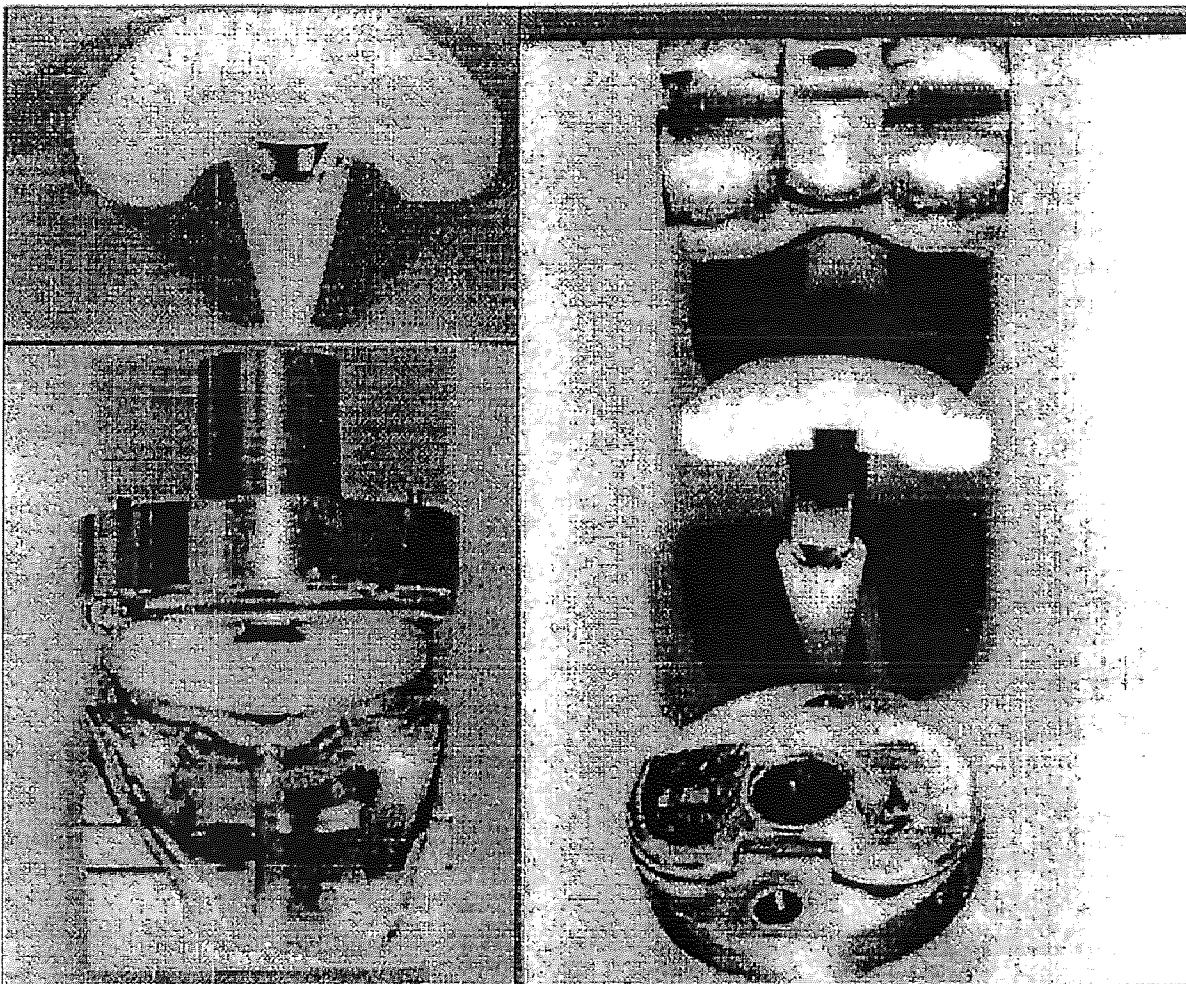


Figure 3.1 LCS A/P Glide Mobile Bearing Knee System [2]

test samples consist of six sets of Anterior/Posterior (A/P) Glide Tibial Bearings. Those bearings were made of Ultrahigh Molecular Weight Polyethylene (UHMWPE). Unlike most knee replacement systems in the United States, the New Jersey LCS® knee replacement systems have a mobile bearing. They show a decrease in contact stress and constraint forces as well as an increase in congruent surface contact.

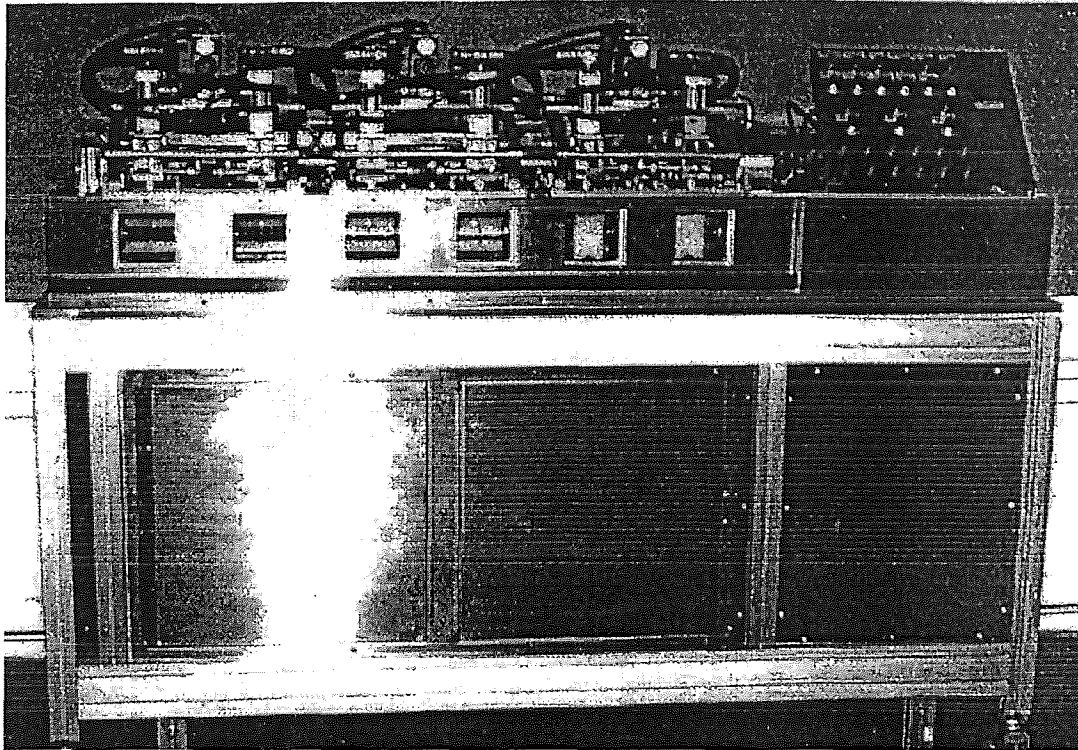


Figure 3.2 New Jersey Mark III Knee Simulator [10]

Each of the knees, which were tested currently, has a conical control arm. It consists of a metal part and an UHMWPE part. These six sets of bearing systems were divided into two groups with three sets per group. Each set of the bearing system of the first group was mounted onto a Cobalt Chromium (Co-Cr) alloy tibial platform with a Cobalt Chromium (Co-Cr) alloy LCS® femoral component. The samples in the first group were numbered as 1, 3, and 5. Each set of the bearing system of the second group was

mounted onto Titanium (Ti) alloy tibial platform with LCS® femoral component, and both coated with Titanium Nitride (TiN) alloy. They were numbered as 2, 4, and 6. All the samples were mounted into the New Jersey Mark III Knee Simulation System.

The New Jersey Mark III Knee Simulator (Figure 3.2) is a six station mechanical testing device used to simulate loading and motion of the knee in order to determine wear and load carrying characteristics of total knee replacement systems. The simulator can be configured to produce a normal walking with gait angle of flexion-extension of 70° and axial rotation of $\pm 6^\circ$. It can also be reconfigured to produce flexion-extension angles from 40° to 90° with 10° intervals by disassembling the main crankshaft and repositioning the connecting rod journal. An axial rotation angle, as large as $\pm 15^\circ$, can be obtained by changing the camshaft. The simulator can be adjusted for peak value, duration, loading and unloading rates. A hydraulic cylinder subsystem is used to produce axial load. Adjusting the control valves can regulate the load magnitude and load rate. A cooling lubrication fluid in each station flows independently by having its own reservoir and filter. The monitor subsystem insures that the cooling lubrication subsystem is functioning properly. Once the fluid level is not maintained at a sufficient level, the system will automatically shut off and a warning light will be lit on the control panel.

Before the simulation, all the reservoirs, which were used to contain the lubrication fluids, were washed with water and then distilled water. All the six test cells were cleaned with alcohol and then rinsed with distilled water. The water filters were changed before the beginning of the simulation. The machine was run for about twenty minutes before the test samples were put into it. So the debris in the tubes of the lubrication system could be washed out.

3.1.2 Loading Condition

The knee simulator uses a hydraulic system to simulate the loading profile. There are six test cells in the simulator. Each two adjacent cells are in one pair. And that pair is called a station. So there are three stations in the machine. For each station there is a hydraulic sub-system, which controls the loading profile for the pertinent station.

Same loading conditions were setup for both the first simulation and second simulation. In the first simulation, one pressure sensor and a storage oscilloscope were used to setup the loading profile. The test was run at an approximated frequency of 2 Hz (exact 1.6 Hz). By adjusting two hydraulic valves in each sub-system and by storing the loading profile, which picked up by the pressure sensor, and comparing to the pre-selected simulated loading profile, the loading condition was setup. Figure 3.3 shows loading conditions, which was used in the previous test. And a comparison between the simulated loading conditions and loading profile of normal walking gait.

In our current test, we tried to setup the machine according to figure 3.3. However, further inspection into our test setup showed that our loading condition had a 180° shifting. The actual loading conditions of this test are presented in the "Discussion".

Because a second pressure sensor was obtained before the second simulation, two pressure sensors were used to setup the loading condition this time. The two pressure sensors picked up the pressure of the hydraulic subsystems and sent the signals back into the oscilloscope through its dual track channels. They were stored there and compared to the pre-selected simulated loading profile. By fine tuning the two hydraulic valves in the knee simulator, the loading condition was setup. Follow the same procedure, the loading conditions for these three stations were setup. Since two stations were setup at the same

time, the conditions for each station could be compared to each other and adjusted, more accurate loading profile were obtained.

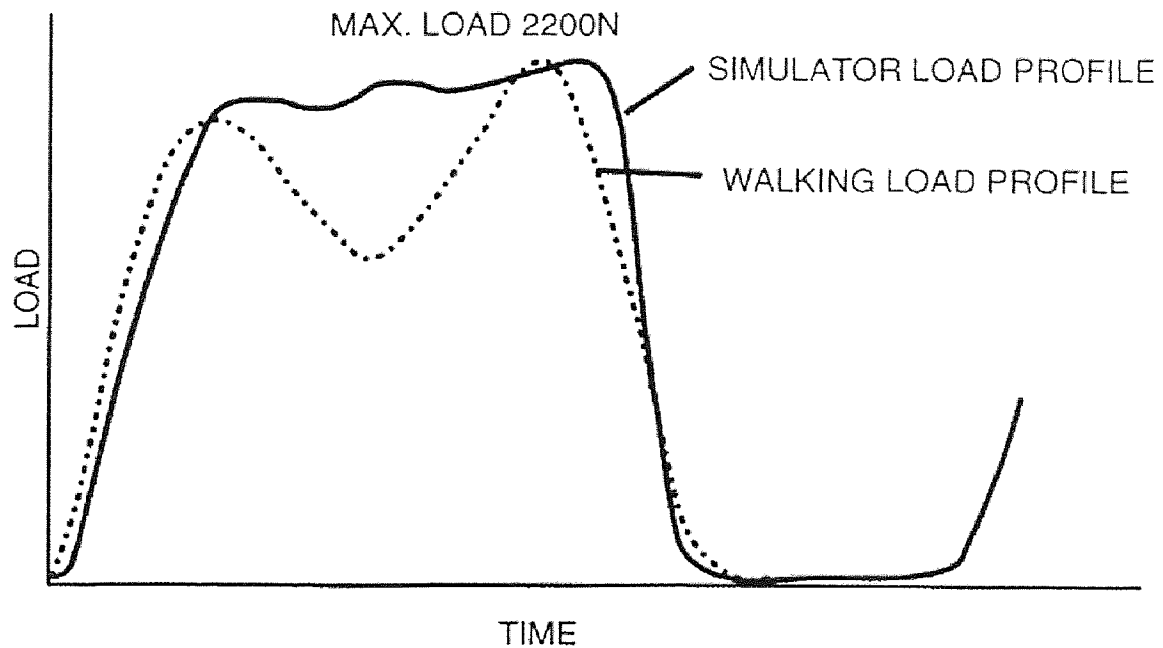


Figure 3.3 Comparison of Normal Walking Profile and Simulated Load Profile [10]

3.1.3 Pre-process of Samples

All the articulating surfaces of metallic components, including the femoral components and the tibial platforms, were polished to a 0.05-micrometer finish and that of all UHMWPE components to a 0.81-micrometer finish. Distilled water was used as the cooling lubrication fluid in this test. Six UHMWPE bearings were cleaned in distilled water also. They were then mounted into the workstations of the simulator along with tibial platforms and femoral components.

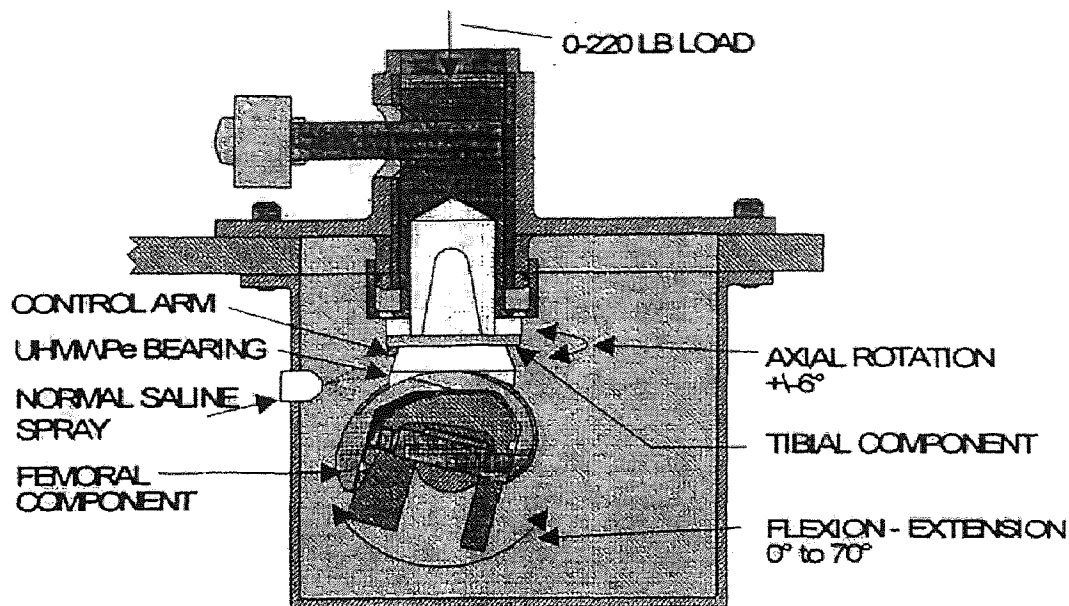


Figure 3.4 Sample Mounted in a Test Cell [11]

The simulator was configured to produce knee flexion angle from 0° to 70° and axial rotation from $+6^{\circ}$ to -6° . (Figure 3.4) This is to simulate a normal gait. The femoral components were mounted to produce an anterior-posterior motion of about 1-cm in length. The simulator runs at an approximate frequency of 2 Hz (actual frequency is 1.6 Hz). The lubrication system keeps the distilled water (lubrication fluid) between the articulating surfaces by spraying it between the bearing and the femoral component and the tibial platform.

The test was setup to simulate a situation without the lateral loading. A center load is applied to the bearing through the femoral component, which simulates the major force performed on the knee joint during a normal walk. The hydraulic cylinder subsystem was set to produce the load which varied from 0 to 1,960N (with corresponding pressure varied from 0 to 440 psi).

3.1.4 Soak Controls

The additional UHMWPE bearings and control arms were prepared. They were needed as soak controls. The amount of weight loss of the bearings was very small. And the sample weight is the major factor involved in determining the wear. The amount of water absorbed by the UHMWPE bearings should be observed and taken into consideration when calculating the weight loss of each bearing. By inserting soak controls into the lubricant reservoirs, weight change due to water absorption can be monitored.

3.1.5 Tibial Bearings' Weight Measurement

The retrievals of components for data collection were scheduled at approximately every 1.0 million cycles. The original weight of the components was measured before any simulation.

During the retrieval, the bearing and the control arm were removed from the test cell as a whole. Prior to weighing each bearing, all components were set on a shelf to dry. The scale used was a Mettler AE 100 high precision electronic balance, which gave measurements in grams to four decimal places. Each component was weighed three times and averaged. [2]

3.1.6 Tibial Bearings' Thickness Measurement

The weight measurement can only tell an overall change in bearings' weight. Then the change in volume was calculated via the UHMWPE density. An additional thickness check

is necessary. It might give some additional information about the wear, which occurred in specific locations.

We predicted that the wear will occur between: (1) the femoral component and the upper surface of tibial bearing (the primary wear), (2) the lower surface of tibial bearing and the tibial platform (the secondary wear), (3) the bearing slot and the control arm, and (4) the control arm and the control arm holder in the tibial platform.

The upper surface of the tibial bearing is a curved surface. The primary wear is predicted to occur at this location. The secondary wear should be occurred between the bottom surface of the tibial bearing and the tibial platform. However, the secondary wear predicted is much less than that at the primary articulating surface. [12] Thus the effect of wear at the secondary articulating surface does not play a major factor on wearing. [12] The wears between the bearing and control arm, and that between the control arm and control arm holder, do not play a major factor on wearing because the contact area between those surfaces is large and stable. So the contact stress between them is low.

On the primary articulating surface of the tibial bearing, two major measure locations were selected. They were at the lowest points on the articulating surface. During the measurement, the bottom surface of the bearing, which was the secondary articulating surface, was served as the datum plane i.e. the reference plane. The tibial bearing was set on a measure platform with the secondary surface facing downward. The dial gauge was fixed on the measure platform with the probe pointing downward. The dial gauge was set on zero with its probe touching the measure platform. Then the tibial bearing was placed under the dial gauge and the probe touched the primary surface. The bearing was then moved around the probe so that the lowest point can be determined. On the dial gauge the

smallest reading is the thickness of the bearing at the lowest point of its primary surface. The measurement was performed three times and the results were averaged for each location.

3.1.7 Making of Repro-Rubber Molds

Reinforced Repro-Rubber mold was made for the primary articulating surface of each bearing before the simulation began. The same procedure was performed after the simulation had been completed. Those molds will be used at a later time, as reference for further analysis for the articulating surface before and after the wear tests.

3.2 Simulations

Totally two tests have been performed to test the wear characteristics of New Jersey LCS® knee replacement systems. The first simulation was performed till 1.9 million cycles. After that, a machine problem occurred. The hydraulic oil damaged the soak controls and two of the bearings. The simulation has to be ceased, so the simulator could be repaired. The second simulation was performed after the machine was fixed. It lasts 3.7 million cycles.

3.2.1 Simulation I

During the first simulation test, distilled water was used as the cooling-lubrication fluid. The simulator was setup as described in the chapter of “Experiment Setup”. One set of

bearing was used as soak control. It was inserted into No. 6 lubrication fluid container. And it was measured along with other bearings, which were under test.

The retrievals were performed at 0, 0.629, 1.00, 1.50 and 1.92 million cycles. After that a hydraulic tube exploded. The hydraulic oil leaked into the cooling fluid container. It led to a permanent damage to the soak control bearing. So the test had to be abandoned.

3.2.2 Simulation II

During the second simulation test, the knee simulator was setup as the first simulation test. It was also the same as that was described in the section of “Experiment Setup”. This time, three sets of additional bearings were used as soak controls. If one set of soak controls was damaged because of machine problems, we still have another two sets of bearings could be used for the following tests. Those three sets of soak controls were numbered as 1, 3 and 5. They were put into the respective lubrication fluid containers. The retrieval were made at 0, 1.43, 2.22, 3.00, and 3.70 million cycles. After that an output relay in the Programmable Controller was out of work. That relay was in charge of the loading conditions of the 2nd test station. It caused that the wear rate of the samples in the 2nd station could not be counted accurately. So the 2nd simulation had to be stopped.

3.3 Data Processing Strategy

During the retrieval, the bearing weight was measured. However, the change in weight, which was figured out directly from measuring results, cannot be looked as the weight change due to wear. The bearing weight change due to the water absorption must be taken

into consideration. The raw results came from the direct weight measurement were called as “original weight”. The weight increase due by water absorption was briefly called as “soak control”. That value was obtained by calculating the weight difference of the bearings used as soak controls.

We have the original weight of the soak control bearings. And we have the current weight of the soak control bearings. So we can calculate the weight change due to water absorption. In fact, during the first simulation, we had one soak control bearing. The weight change of that bearing was looked as the weight change due to water absorption for each bearing that was under test. During the second simulation, we averaged the weight changes for those three soak control bearings. The averaged value was looked as the weight change for each bearing, which was under test. The formula used to calculate the water absorption is listed below (3.1).

$$W_s = W_1' - W_0' \quad (3.1)$$

Where, W_s is the weight increase due to the water absorption.

W_1' is the current weight of the soak control bearing.

W_0' is the weight of the soak control bearing that was obtained before any simulation was performed.

When the weight increase due to the water absorption was taken into consideration, the weight of each bearing was called as “true weight”. The further calculations, which lead to “total bearing weight loss”, “bearing weight loss in each interval” and “bearing weight loss rate”, are all based on the “true” weight of each bearing.

The “true bearing weight” was evaluated by the formula (3.2).

$$W_t = W_1 - W_s \quad (3.2)$$

Where, W_t is the “true bearing weight”.

W_1 is the current bearing weight obtained directly from measurement.

W_s is the weight increase due to the water absorption.

The total weight loss of the bearing was evaluated by the formula (3.3).

$$W_T = W_1 - W_0 \quad (3.3)$$

Where, W_T is the current total weight loss of the bearing.

W_1 is the current bearing weight obtained directly from measurement.

W_0 is the original weight of the bearing, which was obtained before any simulation was performed.

The “bearing weight loss in each interval” was evaluated by the formula (3.4).

$$W_i = W_{t2} - W_{t1} \quad (3.4)$$

Where, W_i is the bearing weight loss in each interval.

W_{t2} is the current “true” bearing weight.

W_{t1} is the “true” bearing weight obtained last time.

The “weight loss rate” was evaluated by formula (3.5).

$$r = \frac{W_i}{n} \quad (3.5)$$

Where, r is the bearing weight loss rate.

W_i is the bearing weight loss in the very interval.

n is the running cycles in that interval.

The volumetric loss of the bearings can be calculated by introducing the density of UHMWPE. It is calculated by formula (3.6). Also the volumetric loss in each interval and the wear rate in volume can be figured out by formula (3.7) and (3.8), respectively.

$$V_T = \frac{W_T}{p} \quad (3.6)$$

Where, V_T is the total volumetric loss of the bearing.

W_T is the current total weight loss of the bearing.

p is the density of UHMWPE. ($p=0.93g/ml$)

$$V_i = \frac{W_i}{p} \quad (3.7)$$

Where, V_i is the total volumetric loss of the bearing in each interval.

W_i is the weight loss of the bearing in the current interval.

p is the density of UHMWPE. ($p=0.93g/ml$)

$$R = \frac{W_i}{p} \quad (3.8)$$

Where, R is the wear rate of the bearing in volume.

W_i is the weight loss of the bearing in the very interval.

p is the density of UHMWPE. ($p=0.93g/ml$)

CHAPTER 4

RESULTS

Since the weight loss of the bearings (Appendix C) and weight loss rate of the bearings (Appendix D) were obtained from the original data (Appendix A and Appendix B). The volumetric loss of the bearings can be calculated formula (3.6). The wear rate in volume can also be figured out by formula (3.8).

4.1 Simulation I

Figure 4.1.1 shows the volumetric loss of each primary bearing throughout the first simulation. Five retrievals at 0, 0.6, 1.0, 1.4, and 1.9 million cycles, have been performed. However after the retrieval at 1.4 million cycles, a hydraulic tube exploded. Later measurement on the 5th and 6th samples shows some weight gain (negative volumetric loss). The 2nd sample shows dramatic increase after 1.4 million cycles. A failed rubber seal caused it. Lubrication fluid (distilled water) escaped from that seal till the water container evacuated. And finally that sample was damaged permanently.

Figure 4.1.2 shows the wear rate of primary bearings. The wear rate of the 2nd sample goes up dramatically because of the same reason stated above. The decrease in wear rate of the 5th and 6th samples is caused by the hydraulic problem. The hydraulic oil stuck to those two bearings and could not be removed completely. So when we calculated the average wear rate (figure 4.1.3), they were not included in after 1.4 million cycles. In addition, when we calculated the average wear rate of bearings against TiN types, the 2nd sample was not included in after 1.4 million cycles either.

In figure 4.1.3, wear rates of the 1st, 3rd and 5th samples were averaged to obtain the average wear rate of these bearings which were against Co-Cr types. The 2nd, 4th, and 6th samples were averaged to get that value for those against TiN types. Both of the average rates show a higher value in the start. It may cause by a grinding and fitting mechanism in the beginning.

4.2 Simulation II

The first simulation had to be ceased by that machine problem in hydraulic system. After the machine was fixed. The second simulation was performed. This time three sets of soak control bearings were used.

Figure 4.2.1 shows the volumetric loss of each primary bearing. Figure 4.2.2 shows the wear rate of each primary bearing. The bearings, which were against TiN types, started at a relatively higher wear rates. At the same time, the bearings against Co-Cr types started at a relatively lower wear rates. After about 3 million cycles, the wear rates of the bearings against TiN began to decrease. On the other hand, the wear rates of the bearings against Co-Cr began to increase. After that, no clear trend can be observed.

Figure 4.2.3 shows the average wear rates of the bearings which against Co-Cr types and those against TiN types. Obviously, the average wear rate against of the bearings against TiN types starts at higher value, while the average wear rate of the bearings against Co-Cr types starts at lower value. They exchanged their position after 2.5 million cycles. And then both of them continued to increase.

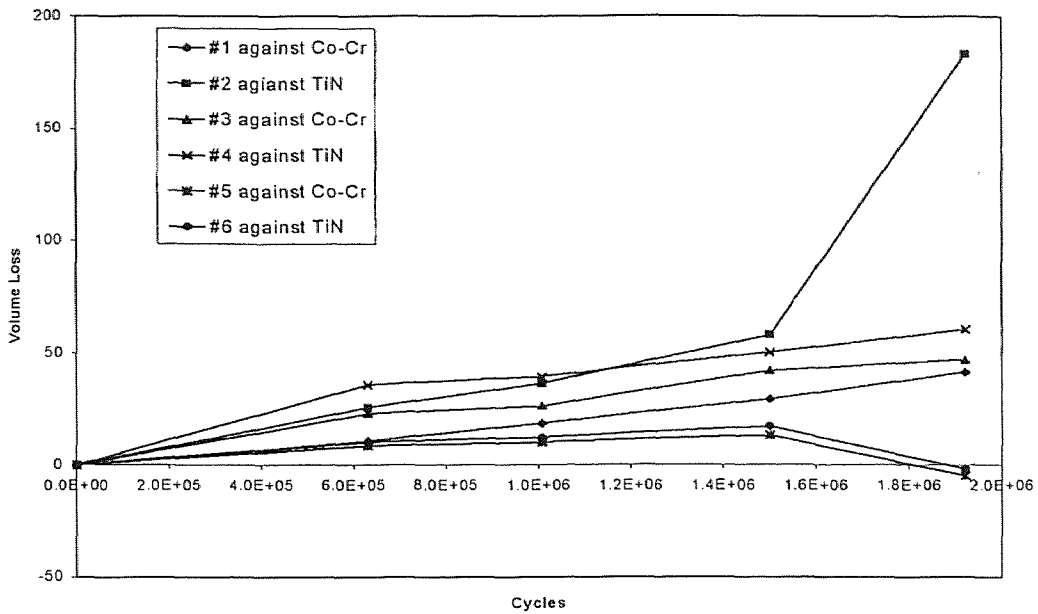


Figure 4.1.1 Bearing Volumetric Loss vs. Running Cycles (unit: cubic mm)

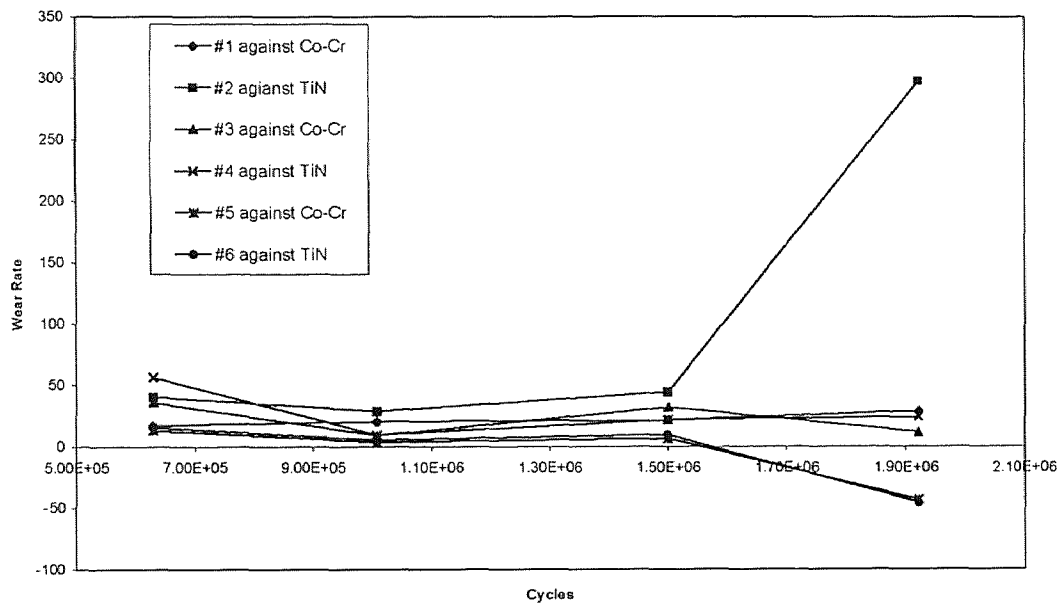


Figure 4.1.2 Bearing Wear Rate in Volume (unit: cubic mm/million cycles)

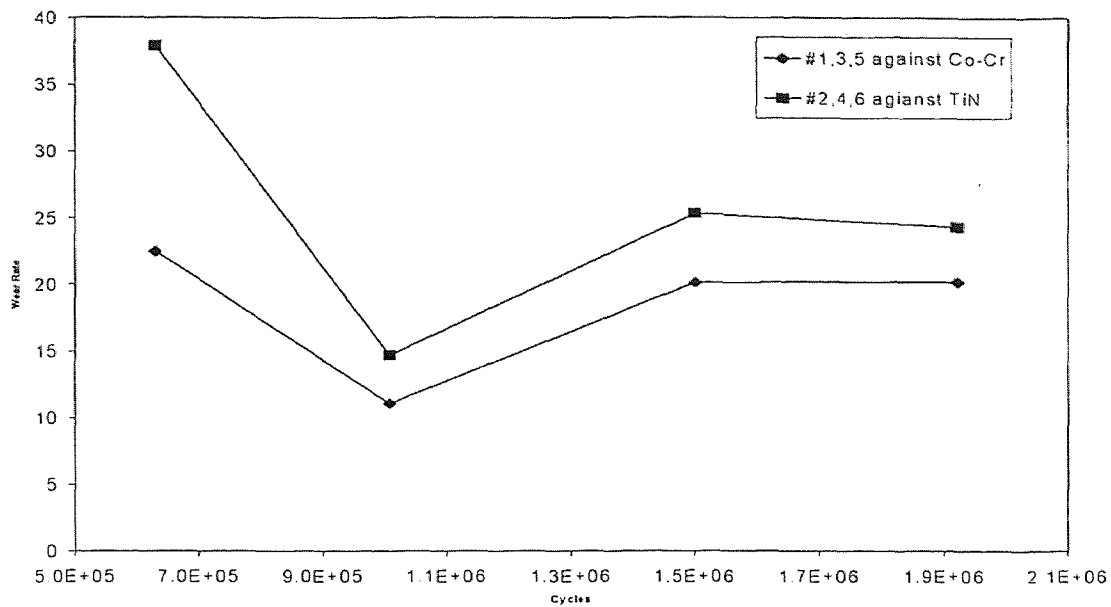


Figure 4.1.3 Average Wear Rate (unit: cubic mm/million cycles)

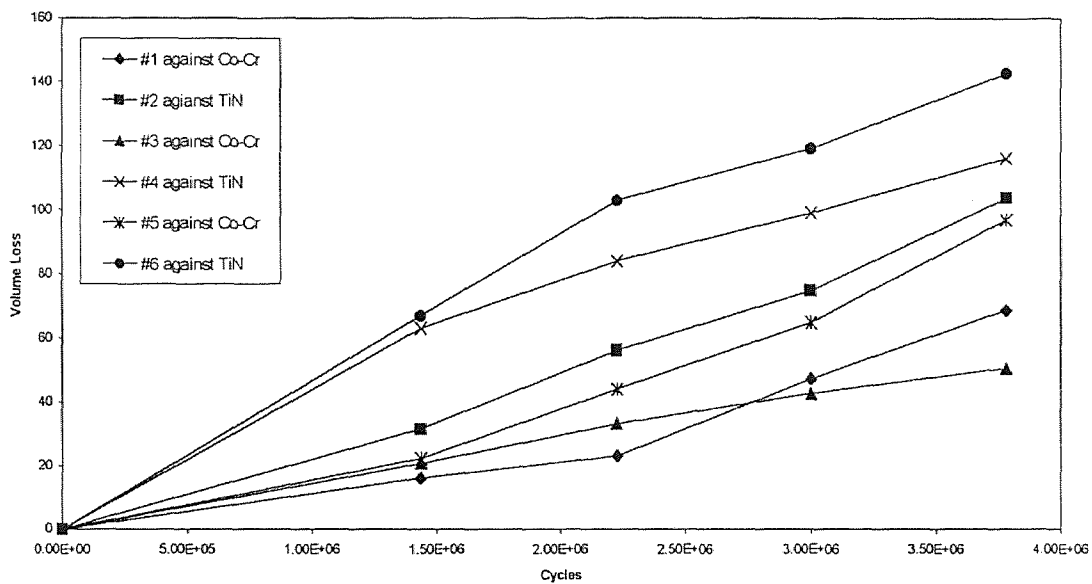


Figure 4.2.1 Bearing Volumetric Loss vs. Running Cycles (unit: cubic mm)

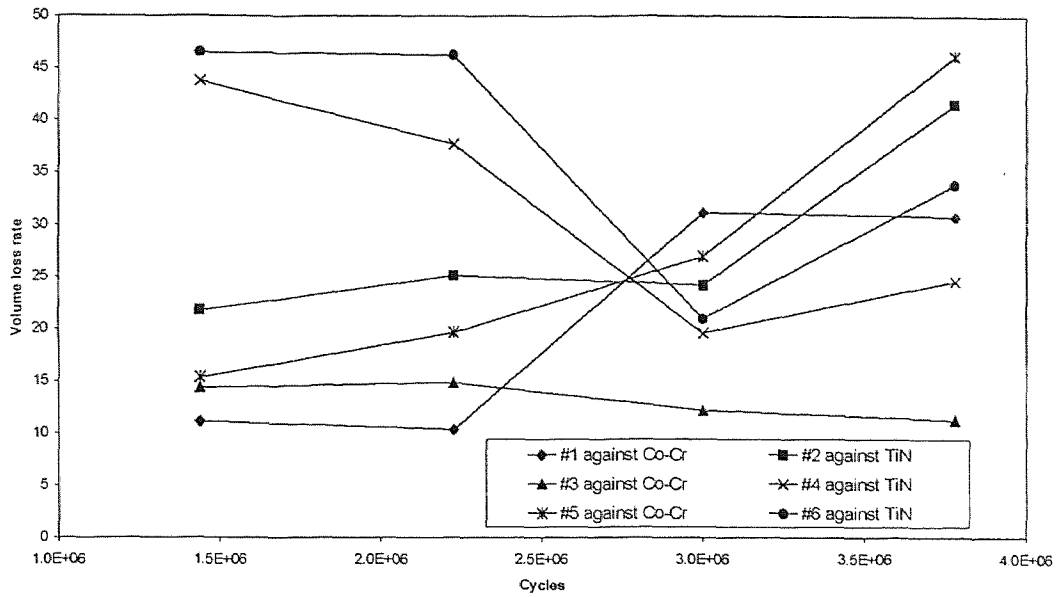


Figure 4.2.2 Bearing Wear Rate in Volume (unit: cubic mm/million cycles)

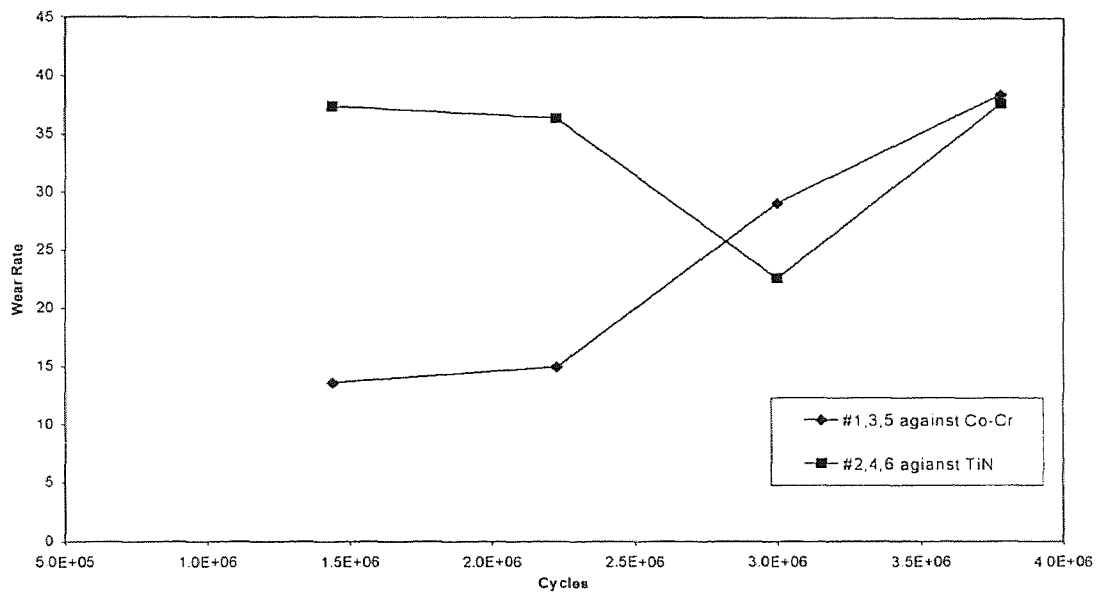


Figure 4.2.3 Average Wear Rate (unit: cubic mm/million cycles)

The thickness of tibial bearings was measured before the beginning of the simulation and after 3.7 million cycles. Table 4.1 and 4.2 show the results of the bearing thickness measurement and the difference in bearing thickness between beginning of the test and the end. It can be seen from these results that the decrease in the thickness on the left side is less than that of right side of these bearings. The 6th bearing is an exception. However we found out later that a screw loosening in the 6th cell. The femoral component went out of its normal mounting position and scratched the bottom of the cell during the flexion-extension motion. The scratch happened at the right side of the femoral component. That means the left side of the component had a higher position than the normal one. That may cause a larger decrease on the left side of the 6th tibial bearing. In the other cells, the bearings showed a higher decrease on the left side than in the right side.

Table 4.1 Thickness of Tibial Bearings at Lowest Locations (unit: inch)

Running cycles	C ₁	C ₁	C ₂	C ₂	C ₃	C ₃
	Left side	Right side	Left side	Right side	Left side	Right side
0	0.2635	0.2655	0.2560	0.2600	0.2640	0.2655
3779726	0.2620	0.2635	0.2510	0.2535	0.2625	0.2630
Decrease	0.0015	0.0020	0.0050	0.0065	0.0015	0.0025

Running Cycles	C ₄	C ₄	C ₅	C ₅	C ₆	C ₆
	Left side	Right side	Left side	Right side	Left side	Right side
0	0.2565	0.2600	0.2575	0.2555	0.2640	0.2655
3779726	0.2515	0.2545	0.2555	0.2525	0.2555	0.2615
Decrease	0.0050	0.0055	0.0020	0.0030	0.0085	0.0040

CHAPTER 5

DISCUSSION

5.1 Bearing Volumetric Loss and Wear Rate

Figure 5.1.1 to figure 5.1.3 were drawn from the results that we obtained from these two simulations. Figure 4.1.1 shows a dramatically increase in the volume loss of the 2nd sample. A loosening rubber seal between the hydraulic cylinder and the station might cause this increase. Some water emitted out from the small gap and then went back. This takes some particles into the lubrication fluid. So additional wear was caused.

The 5th and 6th samples gained some weight during the last wear interval, which is between 1.4 and 1.9 million cycles. This may be caused by the hydraulic oil leakage. It went into the stations, water container and water filters. The hydraulic oil on the surface of the sample could not be completely cleaned out. They affected the measuring results.

From figure 4.1.2, during the first 0.6 million cycles, the wear rates are larger with respect to that of the 1.0, 1.4 and 1.9 million cycle's period. This is due to a decrease in congruence between the femoral component and the bearing platform. A decrease in wear during the second half million cycles (from 0.6 to 1.0 million) is partly due to the gradually decreasing of the congruence progress and partly due to the machine trouble. A key, which transfers rotation between the 2nd cell and the 3rd cell, kept dropping out. A dropping out happened between 629,850 cycles and 1,007,593 cycles. But the machine was still running without extension-flexion motions in the 3rd, 4th, 5th, and 6th cells. So the exact running cycles for these knee bearings in the last 4 cells cannot be determined. Therefore, they had lower running cycles than bearings in the first two cells. However,

when calculating the wear rate, 0.5 million was assumed. Again, a sudden increase in wear rate of the second sample was due to a rubber seal between the hydraulic cylinder and the station loosening. Lubricant water came out and then went back. Some foreign matter entered the cell. They joined the wear and increase the wear rate.

Figure 5.1.1, 5.1.2 and 5.1.3 show the wear rates of the 1st and 2nd samples, 3rd and 4th samples, and 5th and 6th samples, separately. Each two of these samples are put in one pair because they had the same loading profile. From these three figures, we can see that the bearings, which were against Co-Cr femoral components, show a lower wear rate in the beginning. Figure 5.1.1 and figure 5.1.3 show that, between 2.2 million and 3.0 million cycles, the wear rate of bearings against TiN type goes down and those against Co-Cr type goes up. Figure 5.1.1 and 5.1.2 show that the bearings against TiN components have a lower wear rates than those against Co-Cr components. After 3.0 million cycles, figure 5.1.1 shows one trend that the bearing against Co-Cr type has a wear rate lower than that against TiN type. However, figure 5.1.3 shows that the bearing against TiN components has a lower wear rate than that against Co-Cr type. Since both two opposite tendency show out in this interval, further simulation should be performed to obtain a conclusion.

The 3rd bearing, which was against Co-Cr type, keeps showing a low wear rate. We observed hydraulic oil in the water container. It might leak from the hydraulic system. Since hydraulic oil has a better lubrication property than water, the 3rd bearing had an advantage in lubrication over the 4th bearing and even other bearings under test.

We also observed that there are plastic-to-plastic contacts between the lower surface of the bearings and the control arms in the Co-Cr group. However no similar contacts were observed in the bearings against TiN components. The plastic contacts

served as a spring and absorbed certain axial loading. They decreased the wear between the lower surface of the tibial bearing and the tibial platform. In the TiN group, since no such contact was observed. The “pure” metal-to-plastic contacts squeezed out the lubricating water and might affect the wear rate.

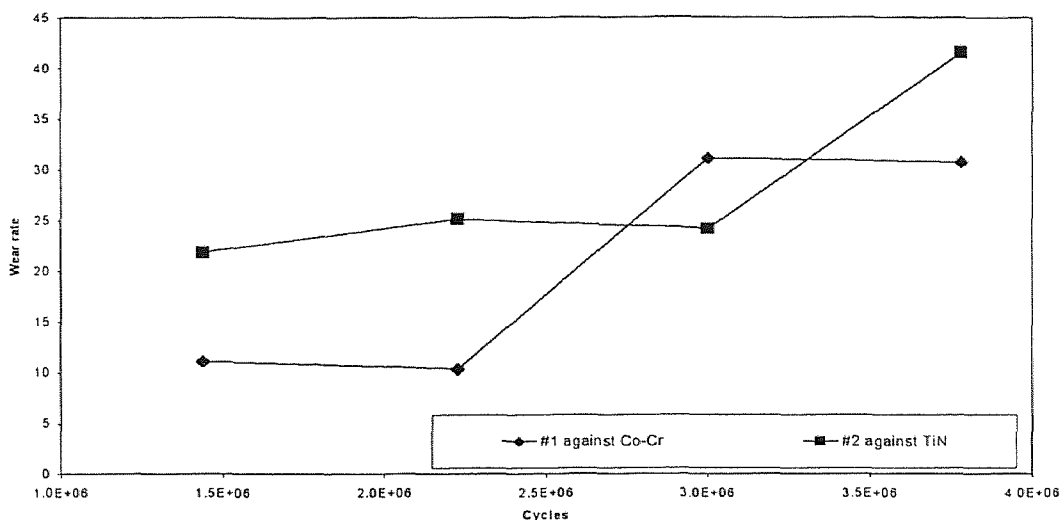


Figure 5.1.1 Wear Rate of the 1st and 2nd Samples (unit: cubic mm/million cycles)

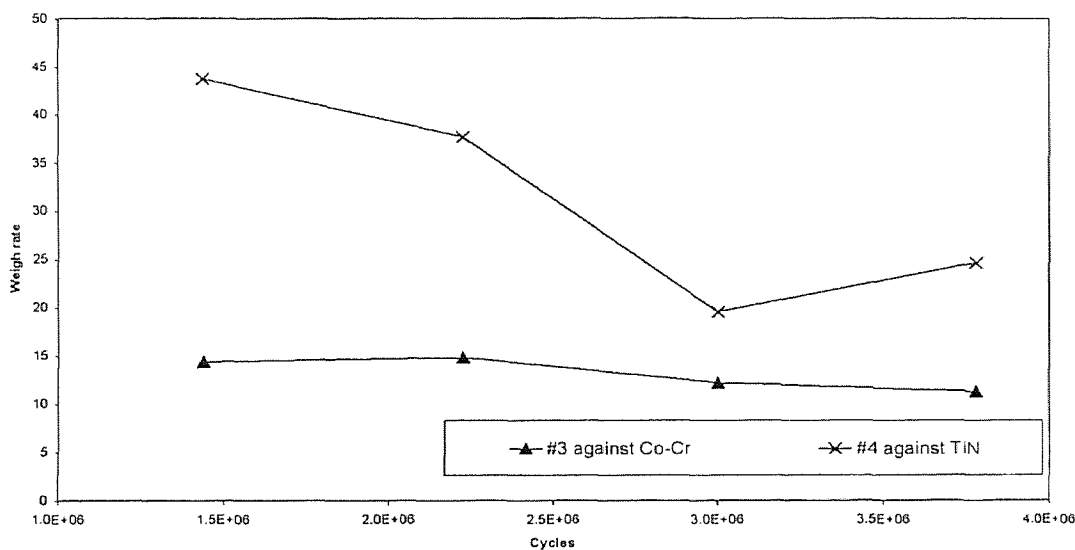


Figure 5.1.2 Wear Rate of the 3rd and 4th Samples (unit: cubic mm/million cycles)

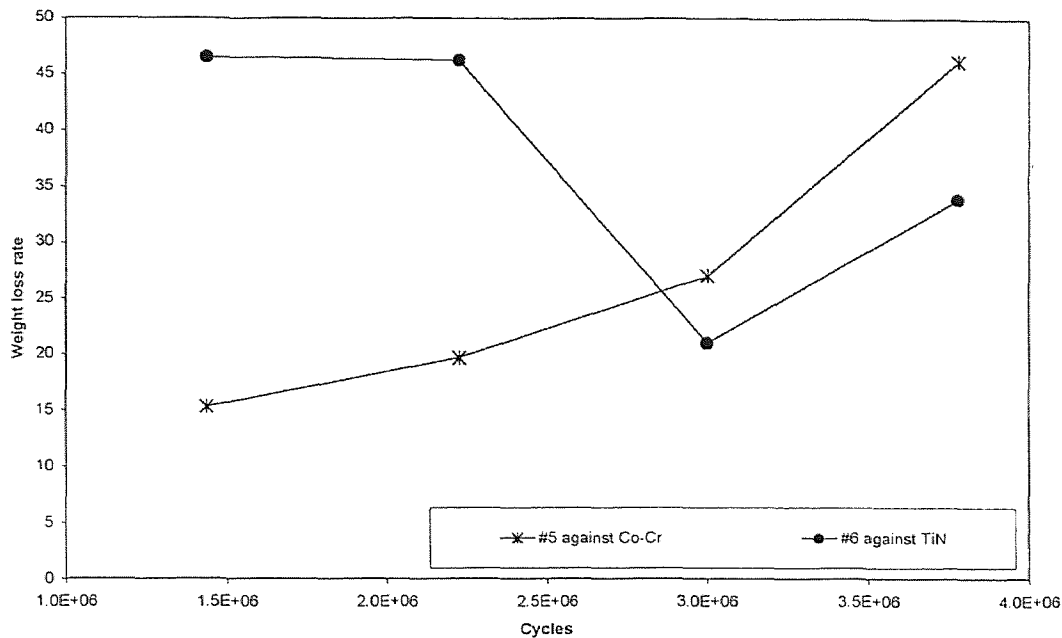


Figure 5.1.3 Wear Rate of the 5th and 6th Samples (unit: cubic mm/million cycles)

5.2 Loading Conditions

The bearing wear is related to the loading profile. Different loading profile may cause different wear results. In the first simulation, two pins, which transferred motion (knee flexion-extension) kept dropping out. They were inserted in time and again. An inappropriate re-insert of the two pins might cause a 180° shift in loading condition. The shifted loading conditions do not represent a simulated normal walking profile. The first simulation was abandoned mainly because of an exploded hydraulic tube. The hydraulic oil permanently damaged sock control and one jag of cooling fluid.

After the knee simulator was repaired, the second simulation was performed. An output relay in the Programmable Controller did not work properly and finally caused the 2nd station lost loading conditions. The machine had to be stopped and repaired again.

Since the test results were not consistent with our prediction and previous study. The experiment setup was inspected. The loading conditions of each station was examined and recorded by a digital oscilloscope. A microscope was used to examine the femoral and tibial components. The radius geometry of femoral components was also measured at specific flexion-extension angles.

Figure 5.2.1, 5.2.2, 5.2.3 show the loading conditions of the 1st, 2nd and 3rd station, respectively. These figures show that, in the second simulation, the loading conditions in each station shifted 180° again. During a normal walking gait profile of an averaged person, the loading profile should begin at around a flexion angle of 0° and end at around 70°. However the loading conditions plotted out by the digital oscilloscope show that the current loading profile begins at around a flexion angle of 70° and end at a flexion angle of 0°. For the knee joint, the best congruency is obtained at 0° flexion and the worst at 90°. Thus under same loading, at 0°-flexion angle, the contact stress is the least. And at 70°-flexion angle in this simulation, the contact stress is largest. The shifted loading conditions exerted maximum load at the worst knee joint congruency. That might greatly increase the wear rate for knee bearings.

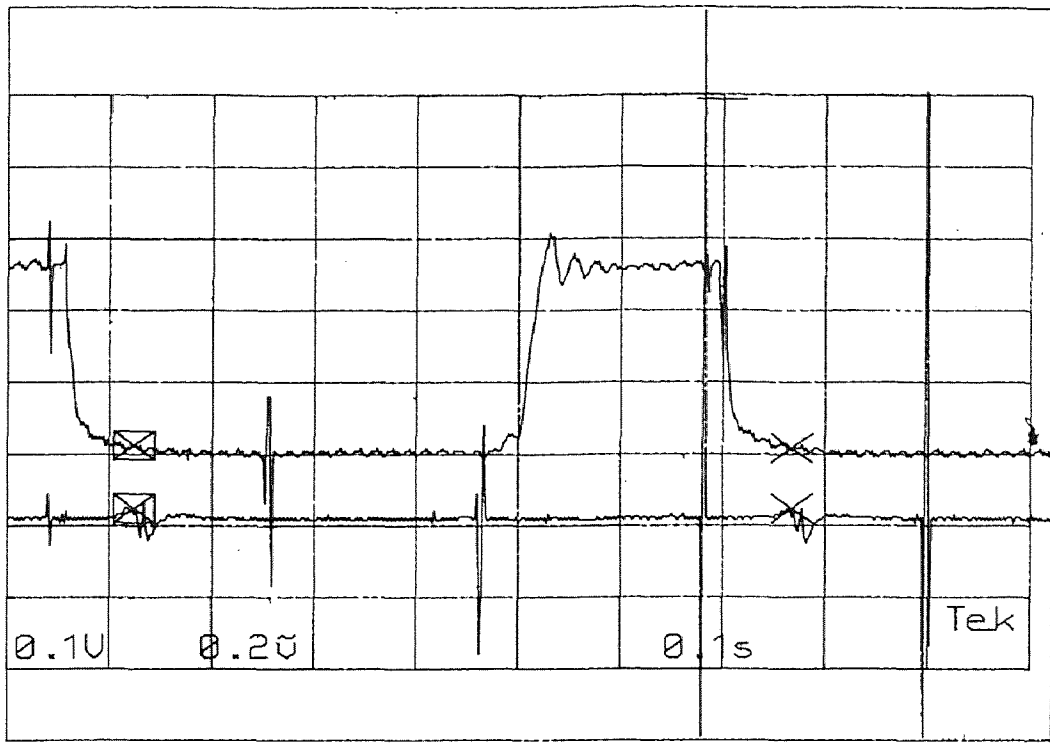


Figure 5.2.1 Loading conditions of 1st station

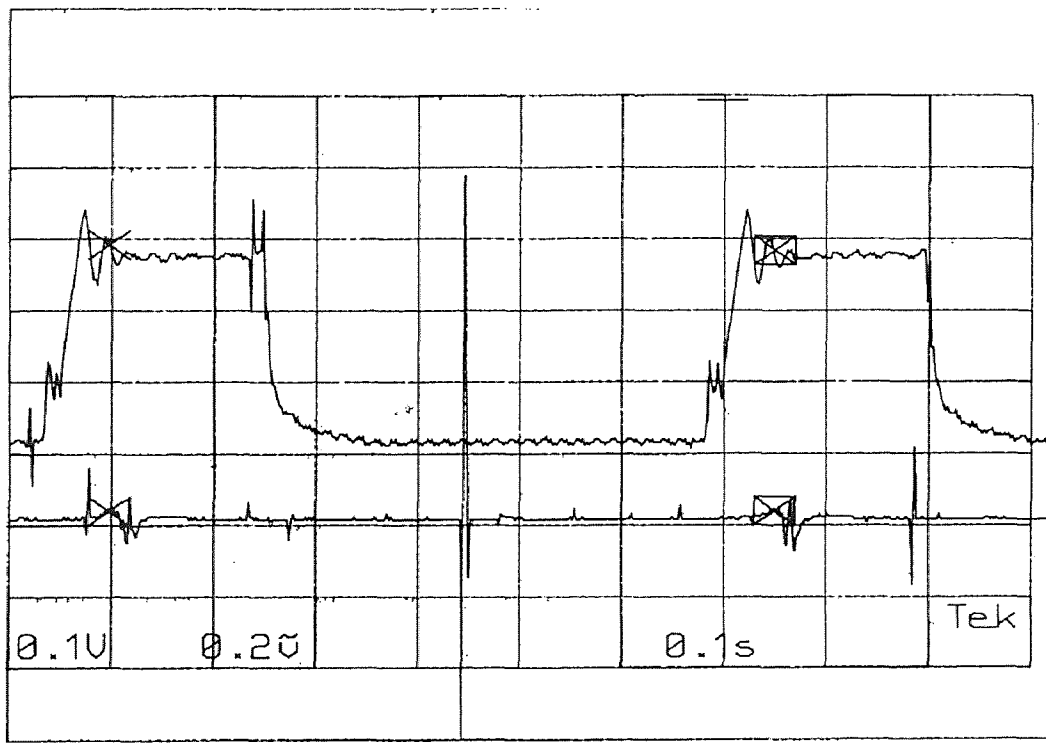


Figure 5.2.2 Loading Conditions of the 2nd Station

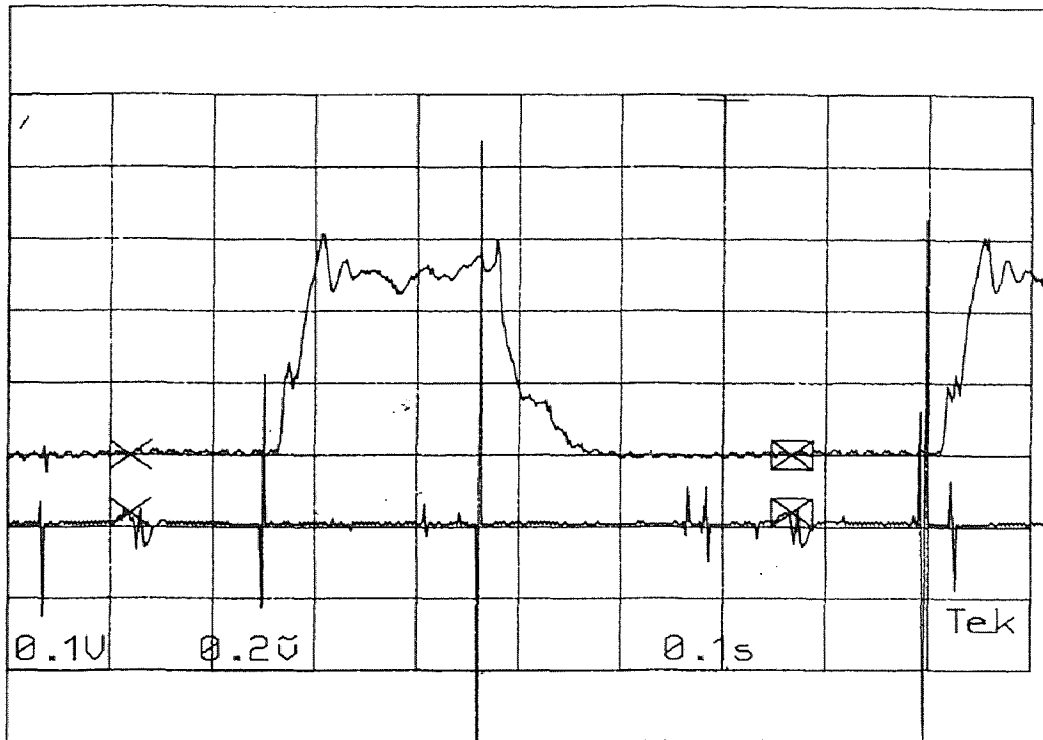
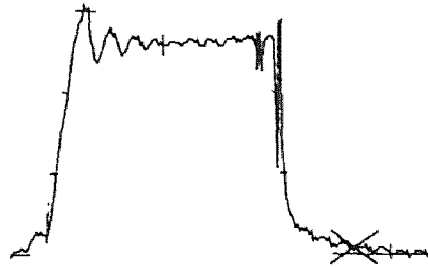


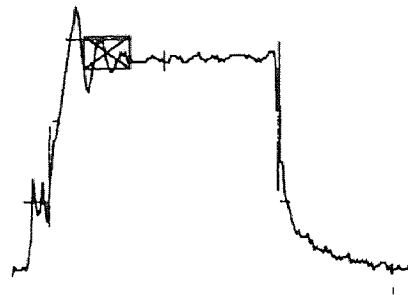
Figure 5.2.3 Loading Conditions of the 3rd Station

Figure 5.2.4 shows a comparison among these three loading conditions in the 1st, 2nd and 3rd station respectively. A careful look into these graphs shows that there are slightly differences in the loading conditions among three stations although they are approximately similar to each other. It can be seen from these graphics that there is a larger peak in both the 2nd and 3rd station than that of the 1st station, when the load is raising. And the load of the 2nd station drops slower than that of 1st station. The load of the 3rd station drops slowest. That might help to explain that the consequence of the bearing volumetric loss is, from largest to the smallest, sample 6, 4, 2, 5, 1, and 3 (figure 4.2.1). Sample 3 is an exception because hydraulic oil was found in its cooling fluid container. The oil might change the property of the cooling fluid. It has better lubrication characteristics and might help to reduce the wear.

Loading conditions of Station I
(Sample 1 and 2)



Loading conditions of Station II
(Sample 3 and 4)



Loading conditions of Station III
(Sample 5 and 6)

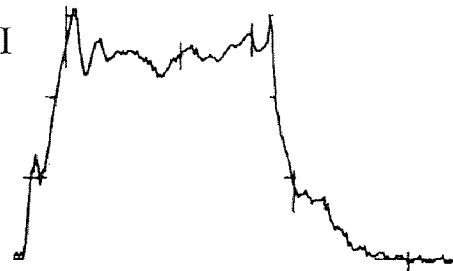


Figure 5.2.4 Comparison of Loading Conditions

5.3 Femoral Component Geometry

The geometry of components might be another factor, which affect the test results. After the 2nd simulation, the geometry of the Co-Cr femoral components and that of the TiN femoral components were measured.

The measurements were made at the flexion angles of 0°, 60° and 75° respectively.

The measurement addressed the radius of femoral components at the bearing articulating

side. Since two values, one is of the left side and another of the right side, were obtained. These two values were averaged. These two radiuses under measurements, articulated with those radiuses of the pertinent UHMWPE bearing. And an ideal radius both for the femoral component and tibial bearing should be 1.511 inch.

If there were differences between those articulating radiuses, there would be a bed-in process. There are two factors should be taken into consideration. The larger the difference in radius between the femoral component and the bearing, the longer the bed-in process is. Further more, for the femoral component itself, the larger the difference in radiuses among these flexion angles, the longer the bed-in process.

Table 5.1 shows the averaged radius of femoral components at the flexion angles of 0°, 60°, and 75°, respectively. The averaged radius of all Co-Cr femoral components is 1.498 inch. The averaged radius of all TiN femoral components is 1.463 inch. And the nominal radius dimension of the tibial bearings is 1.511 inch. That implies that there might be a longer bed-in process for the TiN femoral components than that for the Co-Cr components.

Figure 5.3 shows the averaged radiuses of femoral components in a graphic format. Obviously, as a whole, the TiN group has a common larger difference in radius at different flexion angle in each femoral component than that of the Co-Cr group.

Table 5.1 Averaged Radius of Femoral Components at 0°, 60°, 75° flexion (Unit: inch)

Flexion Angle	C ₁	C ₂	C ₃	C ₄	C ₅	C ₆
0°	1.5041	1.4858	1.4936	1.4476	1.5008	1.4962
60°	1.5148	1.4297	1.4853	1.4384	1.4942	1.4740
75°	1.4970	1.4486	1.4969	1.4777	1.4942	1.4677

Note: C_n is the number of femoral component. It is corresponding to the bearing number.

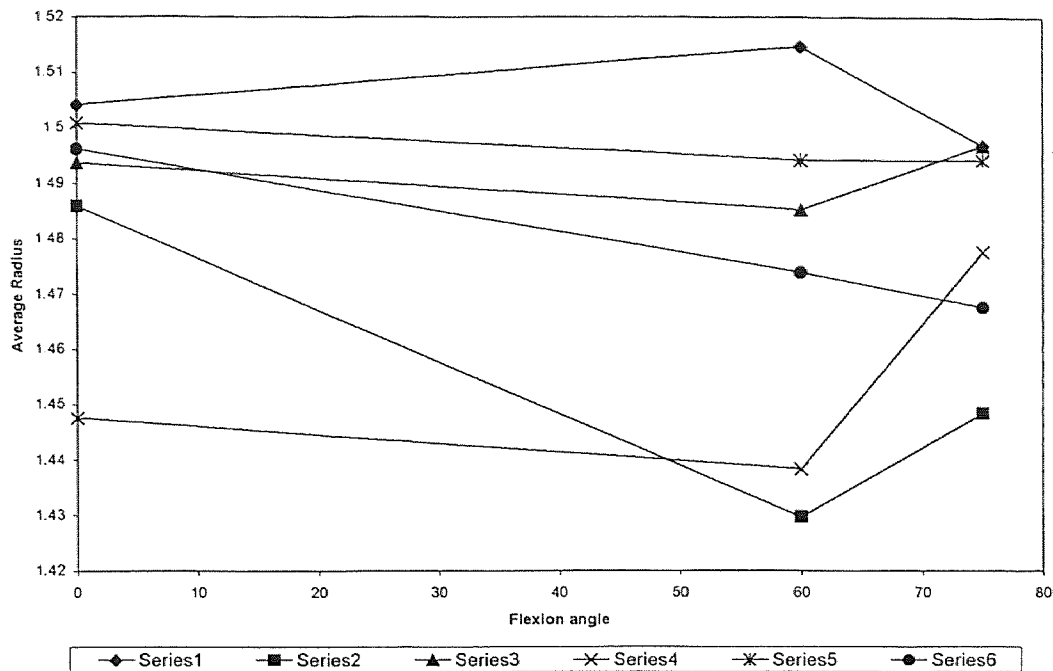


Figure 5.3 Femoral Component Geometry Comparison (unit: inch)

5.4 Cooling-Lubricating Fluid Contamination

We also observed scratches both on the femoral components and tibial platforms. Very hard foreign particles scratch the articulating surfaces between tibial bearing and tibial platform and between tibial bearing and femoral component.

One possible source of the contamination might be the bone cement. The bone cement was used to fix the tested component into its mounting holder. So they could be put into the simulator. Or it might be produced in the machine itself. Or it might come from outside environment.

Further inspection should address the cooling fluid, and the cooling fluid filters. The contamination source should be find out and eliminated.

5.5 Comparison with Previous Simulation Study

In 1995, Alessandro F. Canonaco also performed two simulations on New Jersey LCS® total knee joint replacement systems. UHMWPE bearings on Co-Cr tibial platform and femoral components were tested in the first simulation, with an off-center load. The second simulation tested three Hylamer® and three UHMWPE bearings on Co-Cr tibial platform and femoral components with a center load. Both of the two tests were conducted on New Jersey Mark III knee simulator.

The second test in the previous wear study is similar to the current wear study in the machine setup. However the loading conditions are completely different. Besides the slightly different in hydraulic pressure setup, there is an angle difference of 180° in loading profile. That means, in the previous study, the load began to bear at flexion angle of 0° and remove at 70°. In the current test, the load began to bear at flexion angle of 70° and remove at 0°. Since the load is not constant, and the congruency between the femoral component and tibial bearing decreases from 0° to 70° in flexion angle, the shifting of load conditions might affect the test results greatly.

Previous study shows that an averaged volumetric loss of UHMWPE bearings, which articulated Co-Cr components, is 13 cubic mm at 5.0 million cycles. The current study shows an averaged value of 72.04 cubic mm at 3.7 million cycles for the bearings, which were against Co-Cr components. It is as high as 5.5 times of the previous study, though the running cycles is only as 74 percent of the previous one. The current study also shows an average volume loss of 121.03 cubic mm at 3.7 million cycles for the bearings, which were against TiN components.

CHAPTER 6

SUMMARY

A previous wear study of UHMWPE cups of hip joint replacement systems, which articulate with Co-Cr and TiN coated femoral heads, indicates that the polyethylene bearing against TiN alloy has a lower wear characteristic than that against Co-Cr alloy [11]. The current knee joint wear study was intended to explore the wear characteristic of the UHMWPE tibial bearings, as they articulate with different metal materials and under simulated conditions. In addition, the loading conditions should simulate loading profile of the normal walking gait of an averaged person.

Due to the equipment problems during testing and other factors, like loading conditions did not simulate normal walking gait, femoral component geometry difference, severe contamination of cooling-lubricating fluids, we cannot conclude on the material wear characteristics. On the other hand, it can be seen from the simulation study that: (1) the loading conditions do play a very critical role during the test. A slight difference in loading condition will greatly influence the test results, (2) the geometry of the femoral component is another crucial factor, which will affect the test results.

Any further simulations in the same line with our current study that may provide satisfactory results, must meet the following requirements: (1) the geometry of the components should be the same, (2) the loading conditions must be the same among all the stations, (3) the loading conditions must simulate the profile of a normal walking gait, (4) the contamination of cooling-lubricating system should be corrected, and (5) the entire simulator must be repaired.

CHAPTER 7

RECOMMENDATIONS

Because the wear rate of UHMWPE bearings is very low, the device, which used to measure it, may affect the results. The higher the accuracy of the instrument the higher the precision of the results. As to the measurement of the height of bearings, more locations should be measured. The measuring results obtained this time can not tell if the wear happened in the upper surface or on the bottom. Moreover it cannot tell which one is larger. Some reference marks should be made on the bearing, so they can be used to figure out the exact wear out on the upper surface and on the lower surface.

The loading profile is another important factor, which may affect the test results. There are six cells in the simulation machine. The first two cells constitute the first test station. The second two cells constitute the second station. It is the same to the last two cells. Each of these stations has its own pressure control mechanism. So they have to be adjusted separately and individually. However we just used a pressure sensor and an oscilloscope to ensure the same loading profile to each station. In addition they were used to ensure the same loading profile among all the three stations. It is far from accurate, since the wear of the bearing is so tiny and the number of wear cycles is so large. A little difference in the loading may vary the results greatly. That may be a reason to explain the large difference in the test results among test stations. We strongly suggest a centralized loading profile control mechanism should be engaged. That may reduce the difference in loading profile greatly.

Hydraulic oil is another factor may affect the test results. It kept leaking into the test cells. And they changed the property of lubrication fluids, which should be pure distilled water. The rubber seals in the hydraulic cylinder could be one reason. The aged seals could not prevent the oil from leaking into cells. The machine structure may be another factor. We suggest a side-mounted cylinder mechanism should be used if the machine will be redesign. At least the leaked hydraulic oil cannot take advantage of earth gravity and streamed into the test cell.

Further inspection into bearings and tibial components showed that serious contamination in the cooling systems. Both the bearings and tibial components were scratched by very hard particles. Those particles might come from external environment and might be produced in the system itself. Further inspection into the source of the contamination should be performed.

The power supply of the machine is AC 110 voltage. All the actuation elements use that power directly. We suggest that all elements should use a 24VDC-power supply. That may ensure more safety.

In conclusion, this knee simulator needs to be re-examined. Some of components need to be re-designed. The entire machine needs to be repaired and re-collaborated before any further test studies can be conducted.

APPENDIX A

ORIGINAL DATA FROM SIMULATION I

A.1 Original Data from 1st Retrieval, number of cycles = 0

Table A.1.1 Weight of Primary Bearings: (unit: gram)

Component Number	C ₁	C ₂	C ₃	C ₄	C ₅	C ₆
Weight ₁	20.1844	20.4842	20.1648	20.2873	20.3689	20.5742
Weight ₂	20.1842	20.4842	20.1645	20.2872	20.3686	20.5739
Weight ₃	20.1842	20.4842	20.1646	20.2871	20.3684	20.5739
Average:	20.1843	20.4842	20.1646	20.2872	20.3686	20.5740

Table A.1.2 Weight of Control Arms: (unit: gram)

Component Number	C ₁	C ₂	C ₃	C ₄	C ₅	C ₆
Weight ₁	29.3361	17.6620	28.9526	17.6130	29.1280	17.6293
Weight ₂	29.3360	17.6622	28.9526	17.6129	29.1279	17.6290
Weight ₃	29.3360	17.6620	28.9525	17.6126	29.1279	17.6291
Average:	29.3360	17.6620	28.9525	17.6128	29.1279	17.6291

Weight of Soak Controls:

Table A.1.3 Weight of Primary Bearings: (unit: gram)

Component Number	C ₁
Weight ₁	23.7147
Weight ₂	23.7149
Weight ₃	23.7152
Average:	23.7149

Table A.1.4 Weight of Control Arms: (unit: gram)

Component Number	C ₁
Weight ₁	4.3162
Weight ₂	4.3166
Weight ₃	4.3170
Average:	4.3166

A. 2 Original Data from 2nd Retrieval, number of cycles = 629,850

Table A.2.1 Weight of Primary Bearings: (unit: gram)

Component Number	C ₁	C ₂	C ₃	C ₄	C ₅	C ₆
Weight ₁	20.1876	20.4738	20.1566	20.2673	20.3740	20.5783
Weight ₂	20.1874	20.4738	20.1566	20.2672	20.3739	20.5777
Weight ₃	20.1874	20.4738	20.1566	20.2671	20.3740	20.5775
Average:	20.1875	20.4738	20.1566	20.2672	20.3740	20.5778

Table A.2.2 Weight of Control Arms: (unit: gram)

Component Number	C ₁	C ₂	C ₃	C ₄	C ₅	C ₆
Weight ₁	29.3416	17.6671	28.9783	17.6216	29.1297	17.6313
Weight ₂	29.3416	17.6671	28.9784	17.6215	29.1295	17.6312
Weight ₃	29.3416	17.6671	28.9783	17.6215	29.1296	17.6312
Average:	29.3416	17.6671	28.9783	17.6215	29.1296	17.6312

Weight of Soak Controls:

Table A.2.3 Weight of Primary Bearings: (unit: gram)

Component Number	C ₁
Weight ₁	23.7282
Weight ₂	23.7283
Weight ₃	23.7283
Average:	23.7283

Table A.2.4 Weight of Control Arms: (unit: gram)

Component Number	C ₁
Weight ₁	4.3221
Weight ₂	4.3222
Weight ₃	4.3222
Average:	4.3222

A.3 Original Data from 3rd Retrieval, number of cycles = 1,007,593

Table A.3.1 Weight of Primary Bearings: (unit: gram)

Component Number	C ₁	C ₂	C ₃	C ₄	C ₅	C ₆
Weight ₁	20.1816	20.4651	20.1547	20.2652	20.3740	20.5773
Weight ₂	20.1816	20.4650	20.1547	20.2651	20.3741	20.5772
Weight ₃	20.1817	20.4651	20.1548	20.2651	20.3741	20.5772
Average:	20.1816	20.4651	20.1547	20.2651	20.3741	20.5772

Table A.3.2 Weight of Control Arms: (unit: gram)

Component Number	C ₁	C ₂	C ₃	C ₄	C ₅	C ₆
Weight ₁	29.3417	17.6865	28.9743	17.6261	29.1299	17.6654
Weight ₂	29.3416	17.6865	28.9745	17.6261	29.1299	17.6654
Weight ₃	29.3416	17.6864	28.9746	17.6261	29.1299	17.6653
Average:	29.3416	17.6865	28.9745	17.6261	29.1299	17.6654

Weight of Soak Controls:

Table A.3.3 Weight of Primary Bearings: (unit: gram)

Component Number	C ₁
Weight ₁	23.7293
Weight ₂	23.7298
Weight ₃	23.7298
Average:	23.7296

Table A.3.4 Weight of Control Arms: (unit: gram)

Component Number	C ₁
Weight ₁	4.3223
Weight ₂	4.3225
Weight ₃	4.3225
Average:	4.3224

A.4 Original Data from 3rd Retrieval, number of cycles = 1,500,756

Table A.4.1 Weight of Primary Bearings: (unit: gram)

Component Number	C ₁	C ₂	C ₃	C ₄	C ₅	C ₆
Weight ₁	20.1738	20.4470	20.1423	20.2572	20.3731	20.5748
Weight ₂	20.1737	20.4470	20.1422	20.2573	20.3733	20.5748
Weight ₃	20.1737	20.4469	20.1422	20.2573	20.3731	20.5748
Average:	20.1737	20.4470	20.1422	20.2573	20.3732	20.5748

Table A.4.2 Weight of Control Arms: (unit: gram)

Component Number	C ₁	C ₂	C ₃	C ₄	C ₅	C ₆
Weight ₁	29.3441	17.6651	28.9665	17.6161	29.1303	17.6307
Weight ₂	29.3440	17.6650	28.9668	17.6161	29.1303	17.6307
Weight ₃	29.3439	17.6650	28.9668	17.6161	29.1303	17.6307
Average:	29.3440	17.6650	28.9667	17.6161	29.1303	17.6307

Weight of Soak Controls:

Table A.4.3 Weight of Primary Bearings: (unit: gram)

Component Number	C ₁
Weight ₁	23.7317
Weight ₂	23.7318
Weight ₃	23.7318
Average:	23.7318

Table A.4.4 Weight of Control Arms: (unit: gram)

Component Number	C ₁
Weight ₁	4.3224
Weight ₂	4.3224
Weight ₃	4.3224
Average:	4.3224

A.5 Original Data from 4th Retrieval, number of cycles = 1,921,300

Table A.5.1 Weight of Primary Bearings: (unit: gram)

Component Number	C ₁	C ₂	C ₃	C ₄	C ₅	C ₆
Weight ₁	20.1625	20.3306	20.1378	20.2478	20.3899	20.5925
Weight ₂	20.1625	20.3306	20.1375	20.2478	20.3899	20.5924
Weight ₃	20.1625	20.3301	20.1377	20.2477	20.3900	20.5926
Average:	20.1625	20.3304	20.1377	20.2478	20.3899	20.5925

Table A.5.2 Weight of Control Arms: (unit: gram)

Component Number	C ₁	C ₂	C ₃	C ₄	C ₅	C ₆
Weight ₁	29.3469	17.6677	28.9863	17.6192	29.1423	17.6861
Weight ₂	29.3470	17.6676	28.9862	17.6192	29.1422	17.6861
Weight ₃	29.3469	17.6676	28.9861	17.6192	29.1423	17.6863
Average:	29.3469	17.6676	28.9862	17.6192	29.1423	17.6862

Weight of Soak Controls:

Table A.5.3 Weight of Primary Bearings: (unit: gram)

Component Number	C ₁
Weight ₁	23.7460
Weight ₂	23.7459
Weight ₃	23.7459
Average:	23.7459

Table A.5.4 Weight of Control Arms: (unit: gram)

Component Number	C ₁
Weight ₁	4.3291
Weight ₂	4.3290
Weight ₃	4.3291
Average:	4.3291

APPENDIX B

ORIGINAL DATA FROM SIMULATION II

B.1 Original Data from 1st Retrieval, number of cycles = 0

Table B.1.1 Weight of Primary Bearings: (unit: gram)

Component Number	C ₁	C ₂	C ₃	C ₄	C ₅	C ₆
Weight ₁	20.866	20.095	20.318	20.126	20.056	20.55
Weight ₂	20.865	20.095	20.317	20.125	20.054	20.549
Weight ₃	20.865	20.095	20.316	20.126	20.054	20.550
Average:	20.865	20.095	20.317	20.126	20.055	20.550

Table B.1.2 Weight of Control Arms: (unit: gram)

Component Number	C ₁	C ₂	C ₃	C ₄	C ₅	C ₆
Weight ₁	29.177	17.658	28.848	17.615	28.933	17.692
Weight ₂	29.176	17.658	28.848	17.614	28.933	17.692
Weight ₃	29.177	17.658	28.848	17.616	28.933	17.693
Average:	29.177	17.658	28.848	17.615	28.933	17.692

Weight of Soak Controls:

Table B.1.3 Weight of Primary Bearings: (unit: gram)

Component Number	C ₁	C ₃	C ₅
Weight ₁	20.140	20.190	20.472
Weight ₂	20.141	20.190	20.472
Weight ₃	20.141	20.190	20.472
Average:	20.141	20.190	20.472

Table B.1.4 Weight of Control Arms: (unit: gram)

Component Number	C ₁	C ₃	C ₅
Weight ₁	4.318	4.272	4.320
Weight ₂	4.318	4.273	4.321
Weight ₃	4.318	4.272	4.320
Average:	4.318	4.272	4.320

B.2 Original Data from 2nd Retrieval, number of cycles = 1,438,485

Table B.2.1 Weight of Primary Bearings: (unit: gram)

Component Number	C ₁	C ₂	C ₃	C ₄	C ₅	C ₆
Weight ₁	20.863	20.078	20.311	20.08	20.046	20.5
Weight ₂	20.864	20.079	20.311	20.081	20.048	20.501
Weight ₃	20.863	20.079	20.31	20.079	20.047	20.5
Average:	20.863	20.079	20.311	20.080	20.047	20.500

Table B.2.2 Weight of Control Arms: (unit: gram)

Component Number	C ₁	C ₂	C ₃	C ₄	C ₅	C ₆
Weight ₁	29.181	17.662	28.855	17.613	28.95	17.694
Weight ₂	29.183	17.663	28.855	17.615	28.951	17.694
Weight ₃	29.182	17.662	28.855	17.614	28.95	17.693
Average:	29.182	17.662	28.855	17.614	28.950	17.694

Weight of Soak Controls:

Table B.2.3 Weight of Primary Bearings: (unit: gram)

Component Number	C ₁	C ₃	C ₅
Weight ₁	20.153	20.203	20.487
Weight ₂	20.152	20.204	20.484
Weight ₃	20.152	20.203	20.486
Average:	20.152	20.203	20.486

Table B.2.4 Weight of Control Arms: (unit: gram)

Component Number	C ₁	C ₃	C ₅
Weight ₁	4.321	4.276	4.325
Weight ₂	4.32	4.275	4.324
Weight ₃	4.318	4.273	4.323
Average:	4.320	4.275	4.324

B.3 Original Data from 3rd Retrieval, number of cycles = 2,227,323

Table B.3.1 Weight of Primary Bearings: (unit: gram)

Component Number	C ₁	C ₂	C ₃	C ₄	C ₅	C ₆
Weight ₁	20.865	20.064	20.308	20.068	20.035	20.475
Weight ₂	20.864	20.063	20.306	20.068	20.034	20.474
Weight ₃	20.865	20.064	20.307	20.069	20.035	20.475
Average:	20.865	20.064	20.307	20.068	20.035	20.475

Table B.3.2 Weight of Control Arms: (unit: gram)

Component Number	C ₁	C ₂	C ₃	C ₄	C ₅	C ₆
Weight ₁	29.182	17.663	28.855	17.614	28.946	17.692
Weight ₂	29.181	17.662	28.853	17.613	28.945	17.691
Weight ₃	29.182	17.663	28.853	17.615	28.947	17.693
Average:	29.182	17.663	28.854	17.614	28.946	17.692

Weight of Soak Controls:

Table B.3.3 Weight of Primary Bearings: (unit: gram)

Component Number	C ₁	C ₃	C ₅
Weight ₁	20.159	20.213	20.493
Weight ₂	20.159	20.213	20.493
Weight ₃	20.159	20.213	20.493
Average:	20.159	20.213	20.493

Table B.3.4 Weight of Control Arms: (unit: gram)

Component Number	C ₁	C ₃	C ₅
Weight ₁	4.322	4.278	4.327
Weight ₂	4.322	4.278	4.327
Weight ₃	4.322	4.278	4.327
Average:	4.322	4.278	4.327

B.4 Original Data from 3rd Retrieval, number of cycles = 3,001,786

Table B.4.1 Weight of Primary Bearings: (unit: gram)

Component Number	C ₁	C ₂	C ₃	C ₄	C ₅	C ₆
Weight ₁	20.846	20.05	20.302	20.058	20.018	20.462
Weight ₂	20.846	20.05	20.302	20.058	20.019	20.464
Weight ₃	20.846	20.05	20.302	20.058	20.02	20.464
Average:	20.846	20.050	20.302	20.058	20.019	20.463

Table B.4.2 Weight of Control Arms: (unit: gram)

Component Number	C ₁	C ₂	C ₃	C ₄	C ₅	C ₆
Weight ₁	29.182	17.663	28.852	17.614	28.941	17.691
Weight ₂	29.182	17.662	28.852	17.614	28.941	17.692
Weight ₃	29.182	17.663	28.852	17.614	28.941	17.692
Average:	29.182	17.663	28.852	17.614	28.941	17.692

Weight of Soak Controls:

Table B.4.3 Weight of Primary Bearings: (unit: gram)

Component Number	C ₁	C ₃	C ₅
Weight ₁	20.16	20.221	20.493
Weight ₂	20.162	20.222	20.495
Weight ₃	20.161	20.221	20.494
Average:	20.161	20.221	20.494

Table B.4.4 Weight of Control Arms: (unit: gram)

Component Number	C ₁	C ₃	C ₅
Weight ₁	4.321	4.281	4.326
Weight ₂	4.323	4.282	4.328
Weight ₃	4.322	4.281	4.327
Average:	4.322	4.281	4.327

B.5 Original Data from 4th Retrieval, number of cycles = 3,779,726

Table B.5.1 Weight of Primary Bearings: (unit: gram)

Component Number	C ₁	C ₂	C ₃	C ₄	C ₅	C ₆
Weight ₁	20.831	20.028	20.3	20.047	19.994	20.446
Weight ₂	20.831	20.028	20.3	20.047	19.994	20.447
Weight ₃	20.832	20.029	20.3	20.048	19.995	20.447
Average:	20.831	20.028	20.300	20.047	19.994	20.447

Table B.5.2 Weight of Control Arms: (unit: gram)

Component Number	C ₁	C ₂	C ₃	C ₄	C ₅	C ₆
Weight ₁	29.184	17.669	28.858	17.619	28.944	17.695
Weight ₂	29.184	17.669	28.857	17.619	28.944	17.695
Weight ₃	29.185	17.669	28.858	17.62	28.944	17.695
Average:	29.184	17.669	28.858	17.619	28.944	17.695

Weight of Soak Controls:

Table B.5.3 Weight of Primary Bearings: (unit: gram)

Component Number	C ₁	C ₃	C ₅
Weight ₁	20.165	20.226	20.5
Weight ₂	20.165	20.226	20.5
Weight ₃	20.167	20.228	20.5
Average:	20.166	20.227	20.500

Table B.5.4 Weight of Control Arms: (unit: gram)

Component Number	C ₁	C ₃	C ₅
Weight ₁	4.324	4.284	4.33
Weight ₂	4.324	4.284	4.33
Weight ₃	4.325	4.284	4.331
Average:	4.324	4.284	4.330

APPENDIX C

BEARING WEIGHT LOSS vs. RUNNING CYCLES

C.1 Primary Bearing Weight Loss vs. Running Cycles (Simulation I)

Table C.1 Primary Bearing Weight Loss vs. Running Cycles:(unit: gram)

Running Cycles	C ₁	C ₂	C ₃	C ₄	C ₅	C ₆
0	0	0	0	0	0	0
629850	0.010	0.024	0.021	0.033	0.008	0.009
1007593	0.017	0.034	0.025	0.037	0.009	0.011
1500756	0.027	0.054	0.039	0.047	0.012	0.016
1921300	0.039	0.171	0.044	0.056	-0.004	-0.002

Primary Bearing Weight Loss vs. Running Cycles

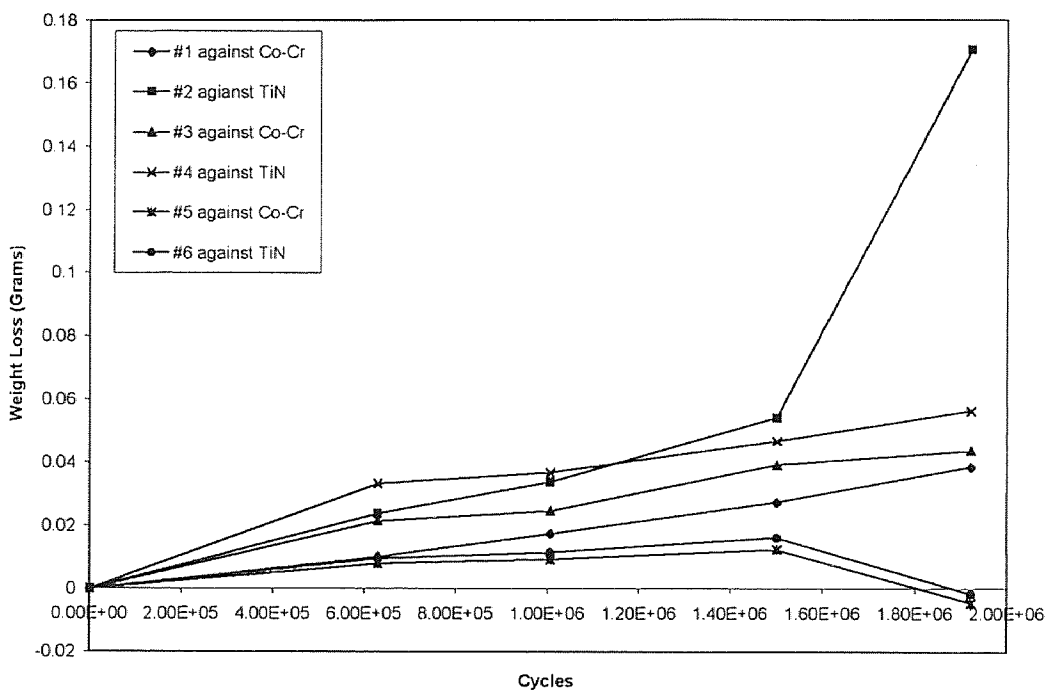


Figure C.1 Primary Bearing Weight Loss vs. Running Cycles (unit: gram)

C.2 Primary Bearing Weight Loss vs. Running Cycles (Simulation II)

Table C.2 Primary Bearing Weight Loss vs. Running Cycles:(unit: gram)

Running Cycles	C ₁	C ₂	C ₃	C ₄	C ₅	C ₆
0	0	0	0	0	0	0
1438485	0.015	0.029	0.019	0.059	0.021	0.062
2227323	0.021	0.052	0.031	0.078	0.041	0.096
3001786	0.044	0.070	0.040	0.092	0.060	0.111
3779726	0.064	0.097	0.047	0.108	0.090	0.133

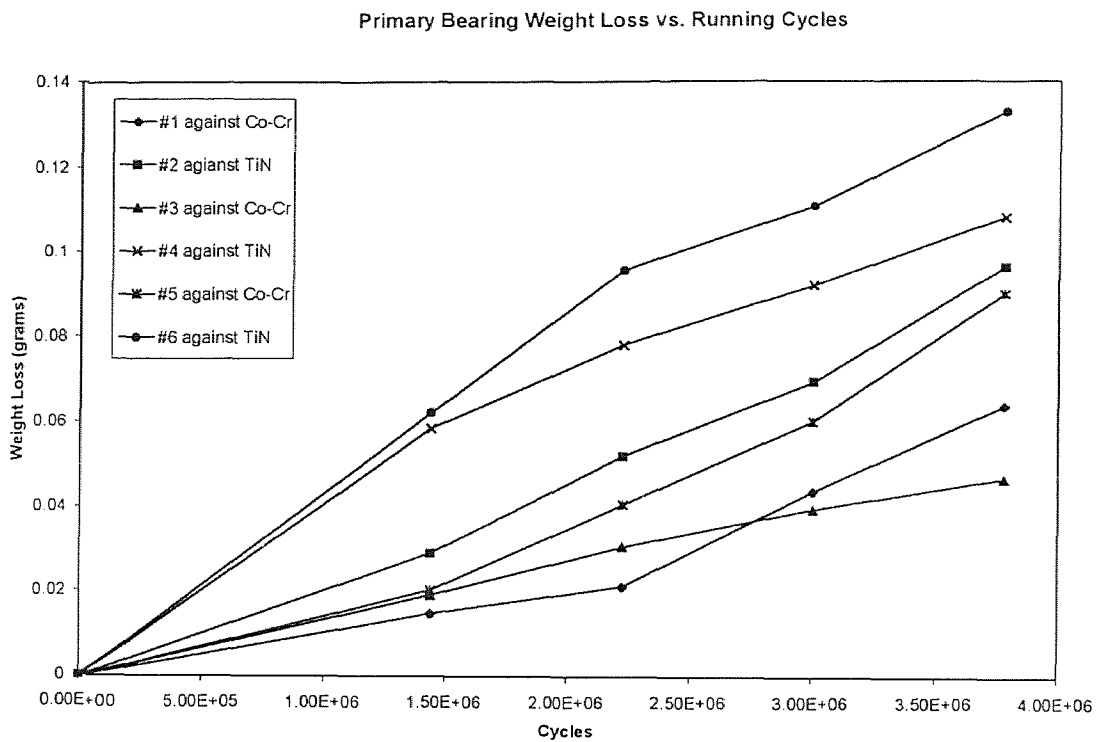


Figure C.2 Primary Bearing Weight Loss vs. Running Cycles (unit: gram)

APPENDIX D

BEARING WEIGHT LOSS RATE vs. RUNNING CYCLES

D.1 Primary Bearing Weight Loss Rate vs. Running Cycles (Simulation I)

Table D.1 Primary Bearing Weight Loss Rate vs. Running Cycles:
(unit: gram/million cycles)

Running Cycles	C ₁	C ₂	C ₃	C ₄	C ₅	C ₆
0	0	0	0	0	0	0
629850	1.609E-02	3.768E-02	3.392E-02	5.292E-02	1.270E-02	1.508E-02
1007593	1.906E-02	2.674E-02	8.560E-03	9.090E-03	3.354E-03	5.207E-03
1500756	2.034E-02	4.103E-02	2.967E-02	2.028E-02	6.150E-03	9.259E-03
1921300	2.671E-02	2.771E-01	1.086E-02	2.259E-02	-3.987E-02	-4.209E-02

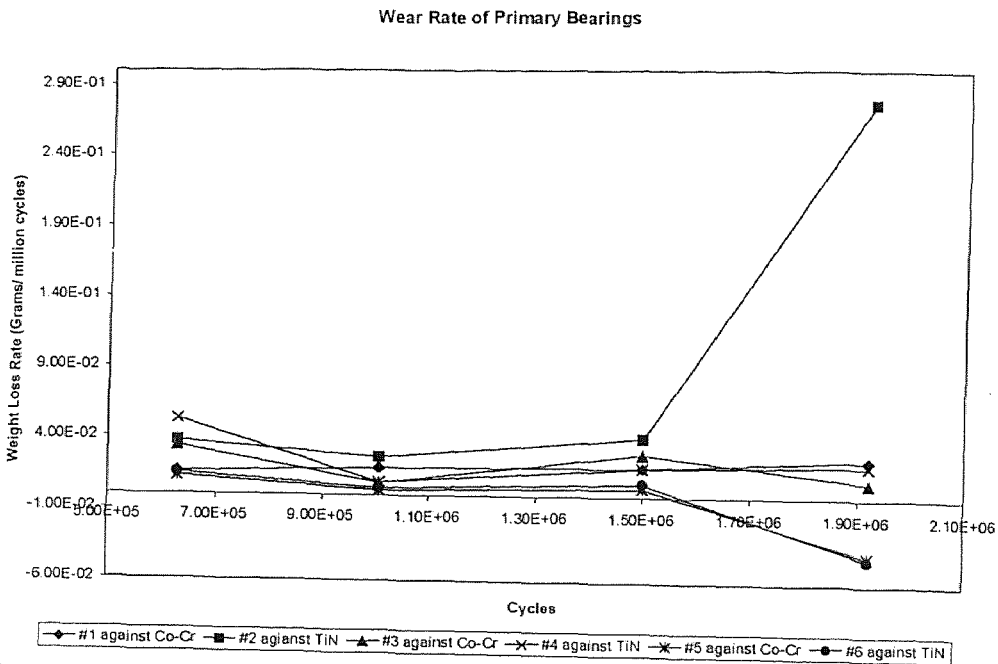


Figure D.1 Primary Bearing Weight Loss Rate vs. Running Cycles (unit: gram)

D.2 Primary Bearing Weight Loss Rate vs. Running Cycles (Simulation II)

Table D.2 Primary Bearing Weight Loss Rate vs. Running Cycles:
(unit: gram/million cycles)

Running Cycles	C ₁	C ₂	C ₃	C ₄	C ₅	C ₆
0	0	0	0	0	0	0
1438485	1.035E-02	2.031E-02	1.336E-02	4.071E-02	1.429E-02	4.326E-02
2227323	9.628E-03	2.340E-02	1.382E-02	3.507E-02	1.831E-02	4.300E-02
3001786	2.898E-02	2.252E-02	1.133E-02	1.822E-02	2.511E-02	1.951E-02
3779726	2.864E-02	3.867E-02	1.050E-02	2.292E-02	4.297E-02	3.151E-02

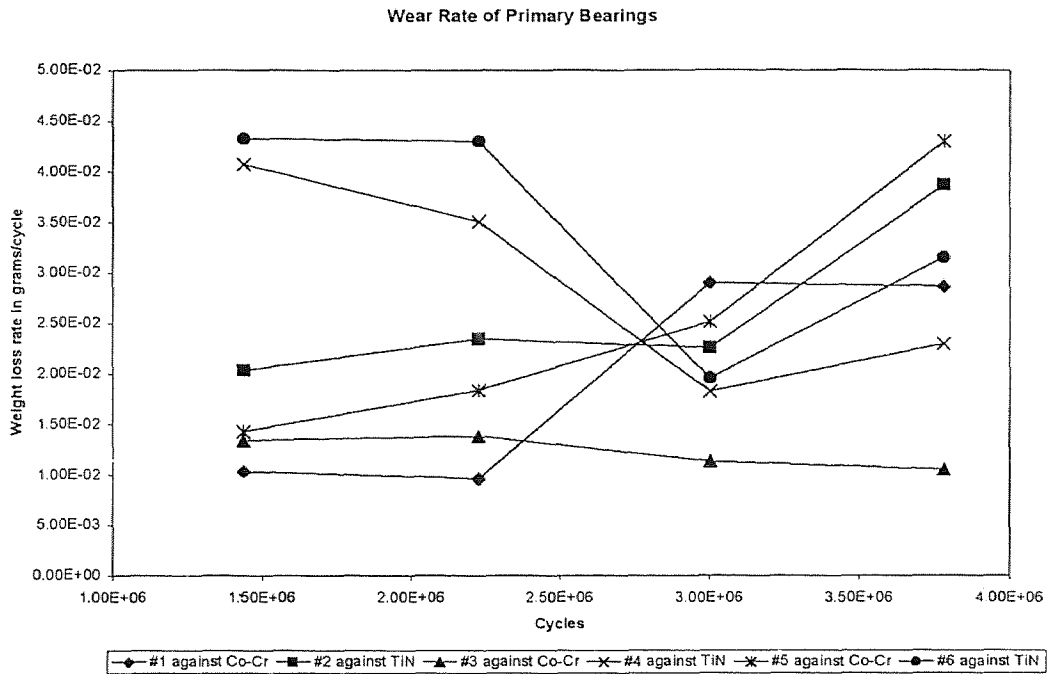


Figure D.2 Primary Bearing Weight Loss Rate vs. Running Cycles (unit: gram)

REFERENCES

1. Van C. Mow and Wilson C. Hayes, *Basic Orthopedic Biomechanics*. New York: Raven Press, 1991.
2. Alessandro F. Canonaco, "Wear of Polyethylene and Hylamer on Cobalt-Chromium: a Knee Simulation Study," M.S. thesis, Biomedical Engineering Program, New Jersey Institute of Technology, January 1995.
3. "Does Gamma Radiation Speed or Slow Wear?" *AAOS On-Line Services*, April 1996, http://www.aaos.org:80/cgi-bin/print_hit...n/april196/biomater.htm?polyethylene+wear (October 1998).
4. "Harris on Primary and Revision Total Hip Replacement Today," *Orthopedics Today*, <http://www.slackinc.com/bone/ortoday/199805/harris.htm> (October 1998).
5. "Elimination of Polyethylene will not Put End to Osteolysis," *Orthopedics Today*, <http://www.slackinc.com/bone/ortoday/199705/osteo.htm> (October 1998).
6. "Polyethylene and Polyethylene Wear," *Wheeless' Textbook of Orthopedics*, <http://www.medmedia.com/o14/13.htm> (October 1998).
7. Daemen Sacomen, etc, "Effect of Polyethylene Particles on Tissue Surrounding Knee Arthroplasties in Rabbits," *Journal of Biomedical Materials Research*, vol. 43, no. 2, pp. 123-129, summer 1998.
8. Michael J. Pappas, and Frederick F. Buechel, "Biomechanics and Design Rationale: New Jersey LCS Knee Replacement System," Depuy Sales Training Seminars, 1993.
9. M. J. Pappas, G. Makris and F.F. Buechel, "Comparison of Wear of UHMWPE Cups Articulating with Co-Cr and Ti-Ni Coated, Titanium Femoral Heads," *Society for Biomaterials Transactions*, vol. 3, May 1990.

10. Michael J. Pappas Ph.D., P.E., “ New Jersey Mark III Knee Simulator System Description and Specifications”.
11. M. J. Pappas, George Makris, “Simulation Study of the Lateral Loading Wear of the LCS A/P Glide Tibial Components,” *Biomedical Engineering Trust*, June 6, 1994.
12. Michael J. Pappas Ph.D., P.E., “LCS White Paper #1. Two Articulating Surface Wear of UHMWPE Bearings,” *Biomedical Engineering Trust*, April 1994.